Improving CAMx GREASD PiG Efficiency

WO 582-11-10365-FY13-09 Final Report

Prepared for:
Doug Boyer
Texas Commission on Environmental Quality
12100 Park 35 Circle
Austin, TX 78711

Prepared by:
Chris Emery, Bonyoung Koo,
Tan Sakulyanontvittaya, and Greg Yarwood
ENVIRON International Corporation
773 San Marin Drive, Suite 2115
Novato, California, 94998
www.environcorp.com
P-415-899-0700
F-415-899-0707

August 2013

ENVIRON

CONTENTS

APPENDICES

TABLES

FIGURES

EXECUTIVE SUMMARY

Photochemical modeling is a complex process involving many supporting models and sub-models to simulate the atmosphere. For example, the CAMx Plume-in-Grid (PiG) sub-model treats the physical and chemical evolution of point source plumes when they are too small to be resolved by a modeling grid. The Greatly Reduced Execution and Simplified Dynamics (GREASD) PiG option is particularly focused on plumes from large NOx sources in which chemistry is controlled by high concentrations of NOx.

This study is the third in a series of PiG evaluation and improvement projects sponsored by the Texas Air Quality Research Program (Yarwood et al., 2012) and the TCEQ (ENVIRON, 2012). In this project, we improved the computational efficiency of GREASD PiG by replacing its use of full photochemical mechanisms (CB05, CB6, or SAPRC99) with a single condensed mechanism that includes a limited number of inorganic reactions that are applicable during early plume stages when high NOx concentrations suppress oxidant production. The new PiG chemistry approach also improves the computational stability of GREASD PiG. With improved stability, we were able to implement revised nocturnal puff growth rates that were developed in the prior TCEQ project. CAMx sensitivity tests were conducted to analyze the effects of the modifications relative to the unmodified version of the model.

The new GREASD PiG chemical mechanism was developed using a box model to emulate puff growth, dilution of emissions, entrainment of ambient background, and gas-phase chemistry. Initial box model tests emulating the original PiG chemical approach with the CB05 chemistry mechanism revealed a growing imbalance in total oxidized nitrogen (NOy), with NOy increasing by up to 30% after 4 simulation hours at night. Some of the excess NOy was NO_2, which could form excess O_3 on the grid the next day. We attributed the lack of nitrogen conservation to the inclusion of ambient background NOy outside the puff for reactions that depend non-linearly on NO_2. Setting the ambient background NOy (including NO_2) to zero eliminated the nitrogen conservation problem. Disregarding background NOy is reasonable for the early stages of NOx plumes because plume concentrations are orders of magnitude larger than ambient NOy. In CAMx, GREASD PiG was modified to ignore ambient background NOy while continuing to entrain background ozone, carbon monoxide, and formaldehyde as the key sources of oxidants to drive the condensed inorganic mechanism.

The new mechanism for GREASD PiG includes 23 gas-phase reactions and it can be run in tandem with any of the photochemical mechanisms used for grid chemistry (CB05, CB6 variants, or SAPRC99). Rate constants and photolysis rates for GREASD PiG reactions are taken directly from corresponding reactions in the grid chemical mechanism, which ensures consistency. Box model tests showed good agreement for NO, NO_2 and O_3 concentrations between the condensed mechanism and CB05. Initial testing in CAMx with MPI and OMP parallelization confirmed correct implementation. In both cases, the new GREASD PiG chemistry mechanism reduced total CAMx runtimes by 10-20% for the 36/12/4 km nested configuration, and by nearly 70% for a single 36 km grid configuration. The tests with MPI took much longer than OMP with the same number of processors because of differences in the

parallelization approaches. We recommend future work to improve the MPI implementation for PiG.

CAMx testing was conducting using pre-existing CB05 modeling datasets. The new GREASD PiG chemistry results in very similar ozone and NOy patterns as the original PiG chemistry. Reduced nighttime puff growth tends to enhance positive ozone concentration impacts from plumes with little change to negative ozone impacts. Reduced puff growth dramatically increases the number of puffs overnight by almost a factor of two while extending average puff ages from about 2 hours to 6 hours. Regardless, CAMx runtimes are only marginally impacted by 1% or less. The effects on NOy are more pronounced for longer-lasting puffs traversing coarser grids (e.g., 36 km) and smaller for finer resolutions where puffs are terminated by size constraints well before meeting chemical constraints.

While we believe that the new PiG chemistry results in a more proper ozone response, we remain concerned that the largest ozone impacts on coarser grids are associated with the lack of interaction between puff-sequestered and background NOy, especially for older, diluted, expansive puffs that cover significant fractions of coarse grid volumes. For that reason, we introduced a new parameter to limit the maximum puff size (and trigger dumping to the grid) that operates similarly to an existing parameter that limits maximum puff age. Puffs can now be terminated when they grow to grid scale (as in the original approach), or when they reach the new maximum size limit, whichever is smaller. We chose to set the default size limit to 10 km based on the conceptual argument that the puff coherency assumption is increasingly invalid approaching and exceeding this scale. This modification led to negligible impact to the ozone results. Given relatively minor ozone impacts from these PiG updates, we verified negligible impact to daily model performance statistics for rural sites throughout east Texas.

CAMx results using the new GREASD PiG were compared to data collected by aircraft in nighttime flights over Texas downwind of the Oklaunion power plant (following Yarwood et al., 2012). The condensed PiG chemical mechanism performed similarly to CB05. Reducing the minimum nighttime horizontal puff growth rates better matched the aircraft-observed plume widths and the chemical conversion of NOx to NOz. Vertical puff spread was well replicated and so vertical puff growth rates were not modified (ENVIRON, 2012). The revised nighttime puff growth rates are implemented in the new GREASD PiG.

ENVIRON is providing the updated CAMx v5.41 code to the TCEQ for additional testing. Appendix A provides an updated CAMx User's Guide section on the PiG submodel that describes the theory and rationale for PiG, physical and chemical treatments, and configuration options.

1.0 INTRODUCTION

The TCEQ uses the Comprehensive Air quality Model with extensions (CAMx) to support State Implementation Plans (SIPs) for Texas' ozone non-attainment areas. Photochemical modeling is a complex process involving many supporting models and sub-models to simulate the atmosphere. For example, the CAMx Plume-in-Grid (PiG) sub-model is used to treat the physical and chemical evolution of emission plumes from point sources when they are too small to be resolved by a modeling grid. The Greatly Reduced Execution and Simplified Dynamics (GREASD) PiG option is particularly focused on the chemistry from large NOx sources.

Previous work supported by the TCEQ and the Texas Air Quality Research Program (AQRP) has identified areas of improvement for the treatment of large NOx point source plumes. This project continues to address those issues, resulting in an enhanced photochemical modeling system for the Texas nonattainment areas.

1.1 Purpose

The purpose of this project was to improve the chemical representation of point source NOx plumes. Specifically, we developed, implemented, and tested a more efficient chemical mechanism for the GREASD PiG sub-model, and addressed several technical inconsistencies with PiG-grid interactions that affect chemical stability and accuracy. With improved PiG stability, we were further able to incorporate reductions to puff growth rates that we had developed in a prior TCEQ project in 2012. CAMx sensitivity tests were conducted to analyze the effects of the modifications relative to the unmodified version of CAMx. Comparisons were made to gauge performance relative to ozone and NOy measurements as available and where feasible.

1.2 Background

Under Project 10-020 of the Texas Air Quality Research Program (AQRP), Yarwood et al. (2012) compared CAMx simulations employing several PiG configurations and a super-high resolution (200 m) flexi-grid against aircraft measurements recorded during multiple transects through the Oklaunion power plant plume on the night of October 10, 2006. That modeling demonstrated the importance of properly characterizing plume dimensions with respect to downwind impacts on next-day ozone. Excessive growth rates lead to over dilution of emitted NOx, excessively rapid reactions with ozone and associated NOz generation overnight, early transfer of plume mass to the grid, and diminished impacts on next-day ozone. As a result of the AQRP work, CAMx v5.40 was publicly released with certain PiG modifications: (1) no explicit shear-induced puff growth during nighttime/stable conditions, (2) minimum puff vertical diffusivities reduced to 0.1 m^2/s, and (3) nighttime stable residual layer reduced from 1000 m to 100 m. Recommendations stemming from that work included adding a user-defined flag to turn off explicit shear growth at all times, and investigating minimum horizontal turbulent energy and length scales in stable environments.

ENVIRON (2012) addressed the AQRP recommendations as part of a series of model updates developed under TCEQ Work Order 12-06. We tested modifications to the PiG growth algorithm, specifically addressing turbulent length scales and minimum (stable) turbulent energy, so that nighttime puff growth rates above the collapsed boundary layer were consistent with aircraft-measured plume widths at 2-3 hour transport times. An important component of those modifications was the addition of a new PiG flag that allows the user to choose to ignore shear effects at all times or only during stable conditions. We then tested the modifications in CAMx sensitivity runs using a preexisting DFW ozone modeling dataset.

Modifications to the PiG growth algorithm led to a significant increase in the number of puffs overnight and in turn the largest and most frequent impacts to surface ozone between midnight and noon each day (typically ±10 ppb). A single obviously faulty PiG-induced ozone impact of 100 ppb occurred at 8:00 AM CST on June 13 in an unmonitored area of east Texas. Given the severity of this event, and our lack of understanding of the cause at the time, we chose not to adopt the changes to PiG growth rates in the subsequent releases of CAMx (v5.41 and v6.00). We instead recommended additional in-depth investigation of PiG chemistry and potentially other improvements to the PiG algorithm to eliminate such faulty behavior. Those recommendations are addressed in this study.

2.0 DEVELOPMENT OF A REDUCED MECHANISM

CAMx has two chemical options for PiG called GREASD and IRON. The first design for GREASD PiG in CAMx version 1.13 employed a condensed chemical mechanism for high NOx conditions that was solved analytically rather than by numerical integration. This approach was computationally efficient but disconnected the PiG chemistry from the grid chemistry. IRON stands for Incremental Reactions for Organics and NOx, and was introduced in CAMx version 4.20. IRON PiG employs the same chemical mechanism as the grid chemistry and includes interactions with grid concentrations through the concept of "incremental chemistry". With the introduction of IRON PiG, GREASD PiG was revised to apply the same chemical treatment but to limit puff lifetime to the initial period when high NOx concentrations suppress oxidant production. GREASD PiG is as chemically complex as IRON PiG, but far less efficient than the first version of GREASD PiG.

In the incremental chemistry approach, puffs carry concentration increments relative to ambient background and these increments can be positive or negative depending on species and stage of puff chemical evolution. Puff chemistry at each time step is first solved for the ambient concentrations in which a puff resides, followed by a second chemistry solution for the total ambient plus puff incremental concentrations. Chemistry is integrated using fully explicit Livermore Solver for Ordinary Differential Equations (LSODE). The updated ambient is then subtracted from the updated total to yield updated puff increments.

Running a full chemical mechanism twice for the relatively small number of active reactions in GREASD PiG is computationally expensive and has not completely eliminated instabilities. Furthermore, the incremental technique has been found to introduce mass errors for total nitrogen according to box model calculations. The objective of this work is to improve the computational efficiency and stability of GREASD PiG by developing a reduced chemical mechanism that is applicable to conditions when high NOx concentrations suppress oxidant production (Karamchandani et al., 1998).

2.1 Test Cases

We created two box-model test cases that apply gas-phase chemistry in combination with dilution and entrainment of ambient air caused by puff expansion. Puff expansion strongly influences chemistry in puffs from NOx emitters by diluting high initial NO concentrations and entraining ambient ozone that converts NO to NO_2 by titration. Puff expansion was modeled as a constant rate of 20% dilution every 15 minutes. Puffs were modeled for 4 hours such that the final concentration of an inert tracer would be diluted to 3.5% of its initial concentration. The ambient air entrained by the puff contained 40 ppb O_3, 1 ppb NOx (as NO_2), 200 ppb CO and 35 ppbC VOC. Emissions were represented by initial concentrations of 450 ppb NO and 50 ppb NO_2 for daytime, and 80 ppb NO and 20 ppb NO_2 for nighttime. Gas-phase chemistry was solved using LSODE with the option to use single or double precision arithmetic; we used double precision because single precision offered no speed advantage. Figure 2-1 shows NO, NO_2 and O_3 concentrations for the daytime and nighttime puff cases with CB05 chemistry.

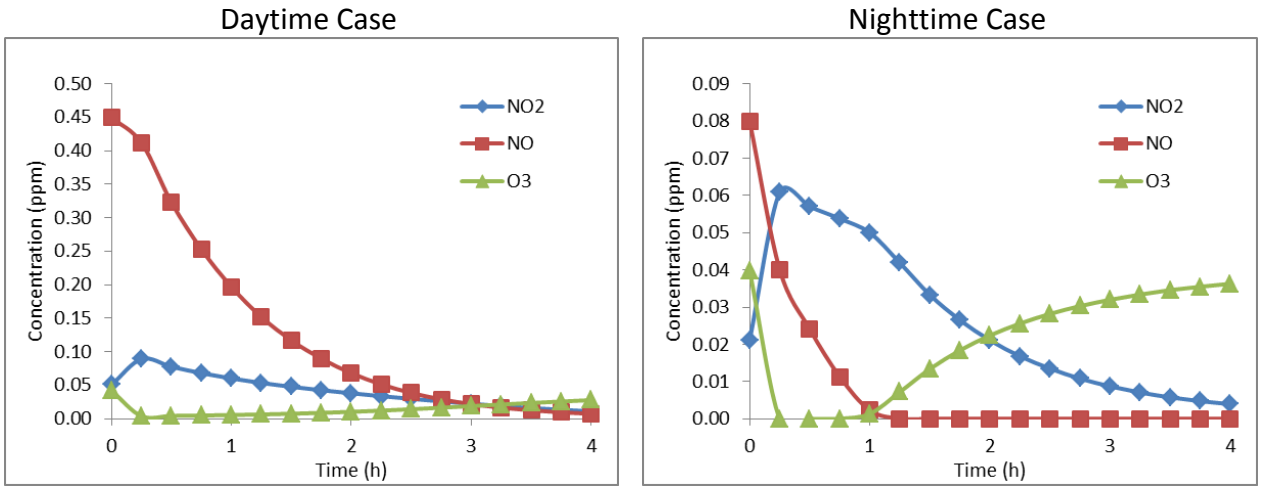

Figure 2-1. NO, NO_2 and O_3 concentrations for the daytime and nighttime puff cases with the CB05 mechanism.

2.2 Nitrogen Conservation

Analysis of the daytime and nighttime puff scenarios modeled with CB05 revealed loss of nitrogen balance, as shown in Figure 2-2. Nitrogen balance is defined as the ratio of puff total oxidized nitrogen (NOy) to the initial puff nitrogen (NOx =NO+NO_2) and balance is achieved when the ratio is maintained at 100%.

For the daytime test, the nitrogen balance started to exceed 100% between hours 2 and 3, and was 106% after 4 hours. In CAMx, GREASD PiG would have slaughtered this puff (i.e., transferred the puff mass to the grid) at ~2.5 hours when the rate of OH reaction with VOCs became larger than the rate of OH reaction with NO_2.

For the nighttime test, the nitrogen balance started to exceed 100% between hours 1 and 2 after the initial NO was depleted and NO_3 began to form, and was 130% after 4 hours. CAMx does not slaughter puffs at night based on chemical criteria and so this puff could have persisted and caused nitrogen non-conservation in CAMx at night. Some of the excess nitrogen is NO_2, which could form O_3 after being transferred to the grid.

We have found that the nitrogen non-conservation results from solving puff chemistry as an increment on top of the ambient background for reactions that depend non-linearly upon NO_2 concentration (e.g., formation of N_2O_5). In these tests the ambient background contained 1 ppb of NO_2. Sensitivity tests with the ambient background NOy (including NO_2) set to zero demonstrated nearly perfect nitrogen conservation as shown in Figure 2-3. The final nitrogen balance in Figure 2-3 is 100.0% for both day and night. Moreover, the production of NOz (HNO_3, N_2O_5, and NTR) occurs at the expense of NO_2 as opposed to being produced on top of erroneously increasing NO_2.

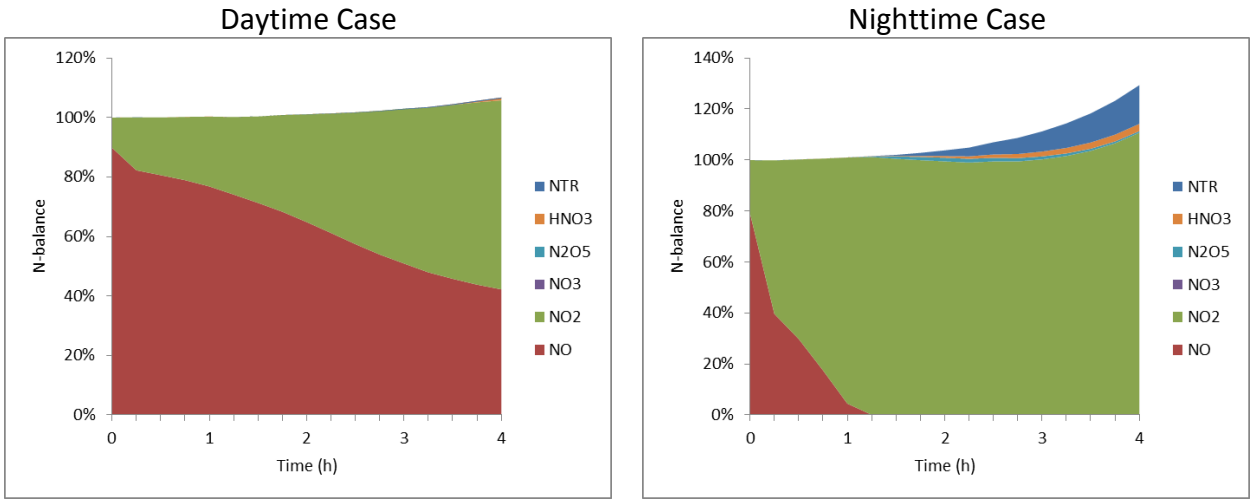

Figure 2-2. Nitrogen balance for the daytime and nighttime puff cases with the CB05 mechanism.

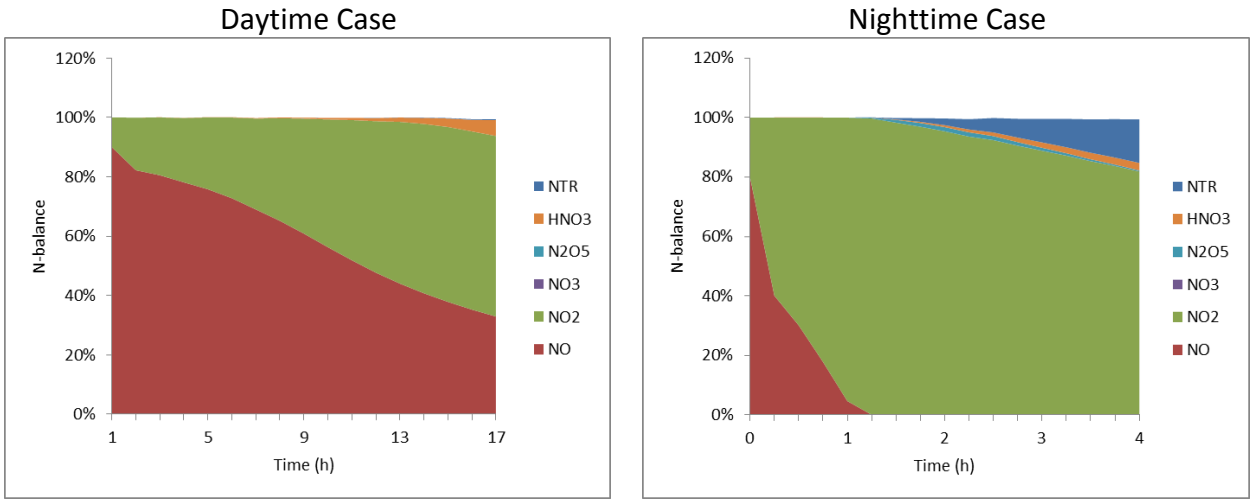

Figure 2-3. Nitrogen balance for the daytime and nighttime puff cases with the CB05 mechanism and the ambient background NOy set to zero.

In CAMx, GREASD PiG was modified to ignore the ambient background NOy while continuing to entrain background ozone, CO, and formaldehyde (HCHO) as sources of oxidants. Assuming zero background NOy is reasonable for the early stages of NOx plumes because puff concentrations are orders of magnitude larger than ambient concentrations. This assumption leads to a model of the main elements of early plume chemistry (Karamchandani et al, 1998) in which emitted NOx reacts with entrained ambient background ozone, leading to chemical reactions that oxidize the NOx to other forms of oxidized nitrogen (NOz).

2.3 Condensed GREASD PiG Chemical Mechanism

The chemical mechanism for GREASD PiG includes 23 reactions listed in Table 2-1 that were selected as follows:

- Reactions for the NO-NO_2-O_3 photo-stationary state established in sunlight (1-3)
- Self-reaction of NO important only at very high NO concentrations (4)
- Production of OH by photolysis of O_3 and HONO in sunlight (5-9)
- Production of nitric acid in sunlight (10)
- Formation of NO_3 and N_2O_5 at night (11-17)
- Production of nitric acid at night (18)
- Production of sulfuric acid in sunlight (19)
- Removal of OH by CO (20)
- Production of OH by photolysis of formaldehyde (21-22)
- Conversion to OH of any HO_2 formed in 20-22 (23)

These reactions dominate gas-phase chemistry in plumes from major NOx emitters in which NOx concentrations are sufficiently high that OH radicals react predominantly with NOx rather than VOCs and consequently oxidant production is suppressed (Karamchandani et al., 1998). The GREASD PiG mechanism is not intended for use in conditions where oxidant production from VOC reactions can occur.

A new diagnostic criterion specific to the condensed mechanism was developed to define the crossover from a NOx-dominant regime to an oxidant production regime, at which point puffs transfer their mass to the grid regardless of puff size relative to the grid. The criterion is based on a radical chain length concept that determines the point at which radical propagation surpasses termination by NO_2:

$$\frac{k_{OH}[SO_2] + k_{OH}[CO]}{k_{OH}[NO_2]} > 1 .$$

Table 2-1 shows the correspondence between GREASD PiG reactions and the complete gas-phase chemical mechanisms implemented in CAMx (CB05, CB6 and SAPRC99). This mapping is used in CAMx to set the rate constants and photolysis rates for GREASD PiG reactions from corresponding reactions in the grid chemical mechanisms. This implementation ensures consistency with these chemical mechanisms.

Figure 2-4 shows good agreement for NO, NO_2 and O_3 concentrations for the daytime and nighttime puff cases between the 23 reaction GREASD PiG mechanism and CB05. The CPU time for the GREASD PiG condensed mechanism was 11% of that for CB05 in these tests.

Table 2-1. List of 23 reactions for GREASD PiG including correspondence to CAMx reaction numbers in the CB05, CB6 and SAPRC99 mechanisms.

Chemical Mechanism for GREASD PIG		Corresponding Reaction Number for Grid Chemistry		
Number	Reaction	CB05	CB6	S99
1	NO2 = NO + O	1	1	1
2	O + O2 + M = O3 + M	2	2	2
3	O3 + NO = NO2	3	3	7
4	NO + NO + O2 = 2 NO2	22	24	10
5 [1]	NO + NO2 + H2O = 2 HONO	23	41	N/A
6	O3 = O1D	9	9	18
7	O1D + M = O + M	10	10	20
8	O1D + H2O = 2 OH	11	11	19
9	HONO = NO + OH	25	43	22
10	NO2 + OH = HNO3	28	45	25
11	NO2 + O3 = NO3	7	26	8
12	NO3 = NO2 + O	14	27	16
13	NO3 = NO	15	28	15
14	NO3 + NO = 2 NO2	16	29	9
15	NO3 + NO2 = NO + NO2	17	30	14
16	NO3 + NO2 = N2O5	18	36	11
17	N2O5 = NO3 + NO2	21	37	12
18 [2]	N2O5 + H2O = 2 HNO3	19	39	13
19	SO2 + OH = SULF + HO2	63	52	44
20	OH + CO = HO2	66	123	29
21	FORM = 2 HO2 + CO	75	97	123
22	FORM = CO	76	98	124
23	HO2 + NO = OH + NO2	30	25	31

1. Rate for GREASD PiG reaction 5 set to zero when used with SAPRC99.
2. Rate for GREASD PiG reaction 18 may be enhanced by reaction on aerosol.

ENVIRON's Chemical Mechanism Compiler (CMC) was used to build the LSODE solver code for the new GREASD PiG mechanism. The new mechanism was installed into CAMx v5.41 for initial testing using the TCEQ June 2006 Rider 8 database. Besides condensing the chemical mechanism, other major chemical modifications in GREASD PiG included: (1) skipping the "background" chemistry step, and (2) excluding all background contributions except for ozone, CO, and HCHO as sources of oxidants. These modifications were not extended to IRON PiG, so that option remains chemically consistent with earlier versions of the model. Finally, minor adjustments were made to the puff mass dumping and wet scavenging algorithms to eradicate

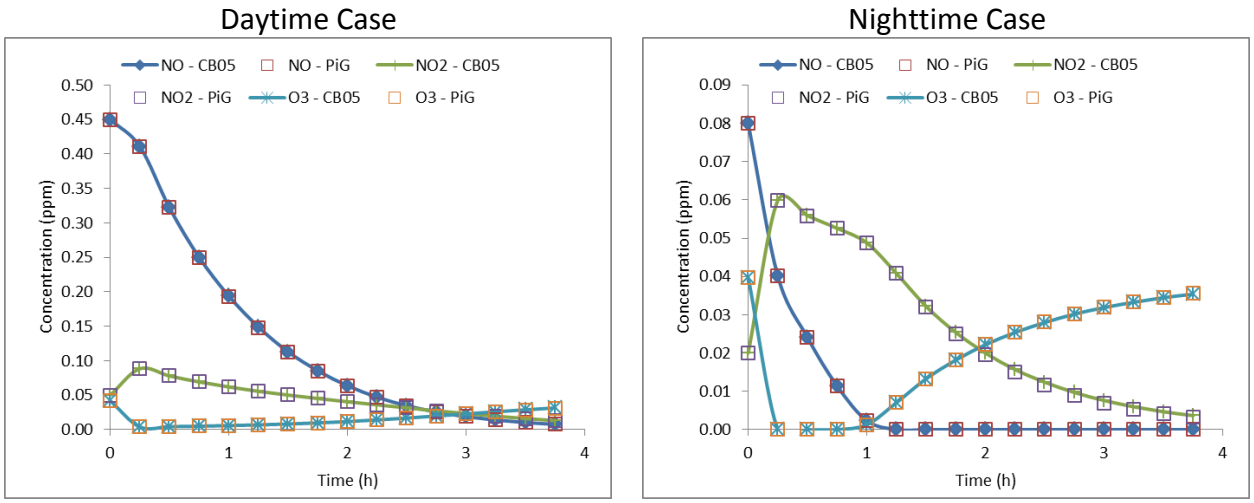

Figure 2-4. NO, NO_2 and O_3 concentrations for the daytime and nighttime puff cases with the 23 reaction GREASD PiG mechanism and CB05.

occasional small errors that we found through initial testing in this project. These final adjustments impact both GREASD and IRON PiG options.

Appendix A provides an updated CAMx User's Guide section on the PiG submodel that describes the theory and rationale for PiG, physical and chemical treatments, and configuration options.

3.0 TESTING PLUME-IN-GRID

Sensitivity runs were conducted to test the new GREASD PiG chemistry mechanism over a wide range of conditions, including:

- The June 2006 TCEQ Rider 8 CAMx dataset;
- The October 10-11 2006 Oklaunion plume CAMx dataset.

Initial testing was first conducted using the TCEQ Rider 8 database to ensure the updated CAMx-PiG system was operating properly. We evaluated speed performance and impacts to ozone and NOy concentrations relative to the standard v5.41 code. We then tested chemical sensitivity and stability to reduced nighttime plume growth rates and elongated plume lifetimes brought forward from TCEQ Work Order FY12-06 (ENVIRON, 2012). Comparisons between the original, condensed, and reduced-growth cases were made against nighttime aircraft data from the October 2006 TEXAQS II aircraft missions. On the basis of these modeling results, one additional PiG refinement was implemented to allow the user to limit puff sizes and force puff dumping in very coarse resolution grids (e.g., >10 km).

3.1 Speed Performance

CAMx v5.41 was run with the TCEQ Rider 8 database with various parallelization and grid configurations to test model runtime impacts from the PiG modifications:

- 3-grid (36/12/4 km) with MPI on 8 CPUs
- 3-grid (36/12/4 km) with OMP on 8 CPUs
- 1-grid (36 km) with OMP on 8 CPUs[1]

Table 3-1 lists the various TCEQ Rider 8 CAMx runs and their naming conventions. Figure 3-1 shows average runtimes for May 31 – June 30 from four key MPI cases. The original PiG (r1m) increases runtime relative to the no-PiG run (r0m) by over 70%. The runtime with PiG chemistry entirely turned off (r2m) is only reduced by ~20%, much less than the total PiG runtime impact. The runtime reduction with the new PiG mechanism (r7m) is ~10%, or roughly half the impact from removing PiG chemistry altogether. It is important to note that these runtimes don't just reflect responses to the amount of chemistry performed, but also reflect the response of the puff populations to different chemistry (e.g., the no-chemistry run leads to longer puff lifetimes and thus more puffs on the grid). Therefore, these runtime impacts are not necessarily linear.

Figure 3-2 shows average runtimes for May 31 - June 15 from four OMP cases. OMP speeds are much faster than MPI by about 100 minutes (~30%) per day using the original PiG. Similarly to the MPI tests, runtimes decrease by ~20% for the case with no PiG chemistry (r2o), but by 17-

[1] The purpose of the single-grid run is described in Section 3.2.

Table 3-1. List of CAMx runs with the TCEQ Rider 8 database to test various PiG, grid, and parallelization configurations. All run names not appended with "36" included the entire 36/12/4 km grid system. The specific tests shown in Figures 3-1 and 3-2 are highlighted.

Run Name	Definition	Parallelization	Duration
r0m	No PiG	MPI 8	May 31 – June 30
r0o	No PiG	OMP 8	May 31 – June 15
r0o36	No PiG, 36K only	OMP 8	May 31 – June 15
r1m	Original PiG	MPI 8	May 31 – June 30
r1o	Original PiG	OMP 8	May 31 – June 30
r1o36	Original PiG, 36K only	OMP 8	May 31 – June 15
r2m	No PiG chemistry	MPI 8	May 31 – June 30
r2o	No PiG chemistry	OMP 8	May 31 – June 30
r5m	No background chemistry, zero background NOy, original PiG chemistry	MPI 8	May 31 – June 30
r6m	Same as r5m, reduced puff growth rates	MPI 8	May 31 – June 30
r7m	New PiG chemistry mechanism	MPI 8	May 31 – June 24
r7o	New PiG chemistry mechanism	OMP 8	May 31 – June 15
r7o36	New PiG chemistry, 36K only	OMP 8	May 31 – June 15
r8o36	New PiG chemistry, reduced puff growth rates, 36K only	OMP 8	May 31 – June 15
r9o	New PiG chemistry, reduced puff growth rates, 10K size limit	OMP 8	May 31 – June 15
r9o36	New PiG chemistry, reduced puff growth rates, 10K size limit, 36K only	OMP 8	May 31 – June 15

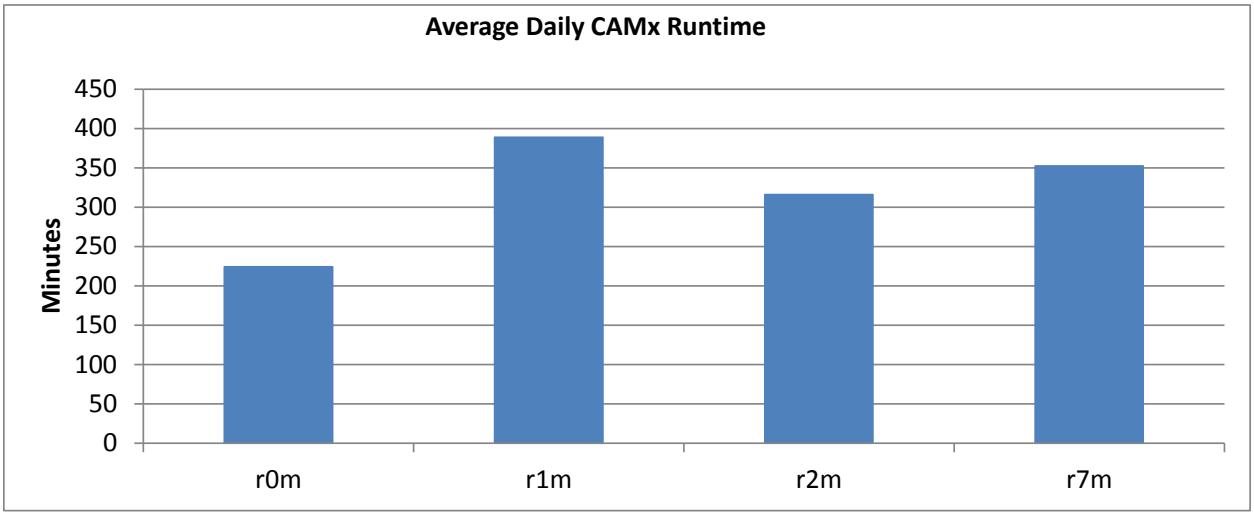

Figure 3-1. Average daily CAMx runtimes (minutes) for the TCEQ Rider 8 database using MPI over 8 CPUs to run the full 36/12/4 km grid system over May 31 – June 30.

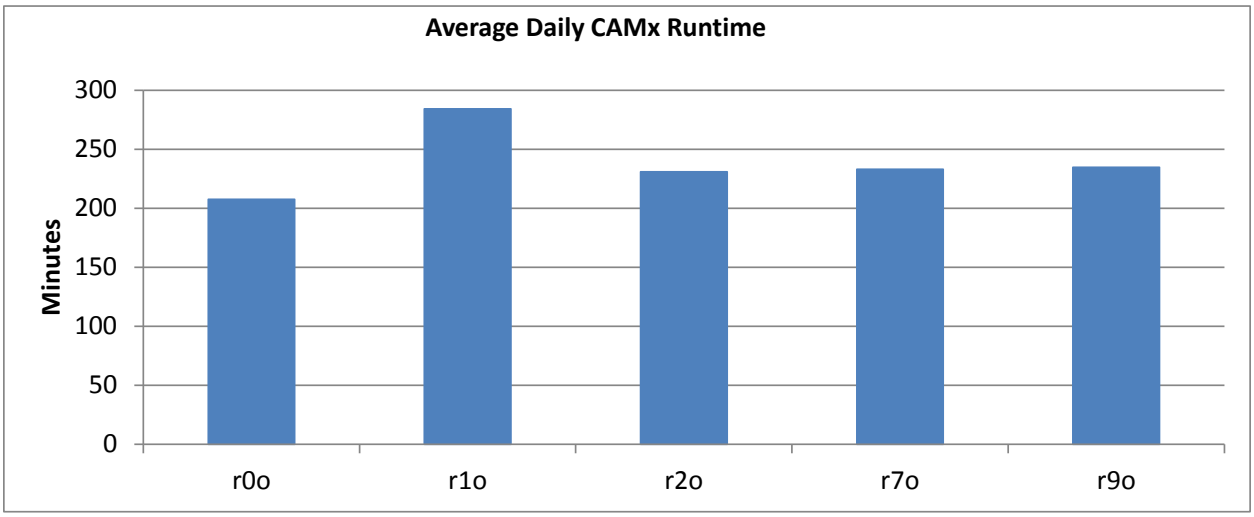

Figure 3-2. Average daily CAMx runtimes (minutes) for the TCEQ Rider 8 database using OMP over 8 CPUs to run the full 36/12/4 km grid system over May 31 – June 15.

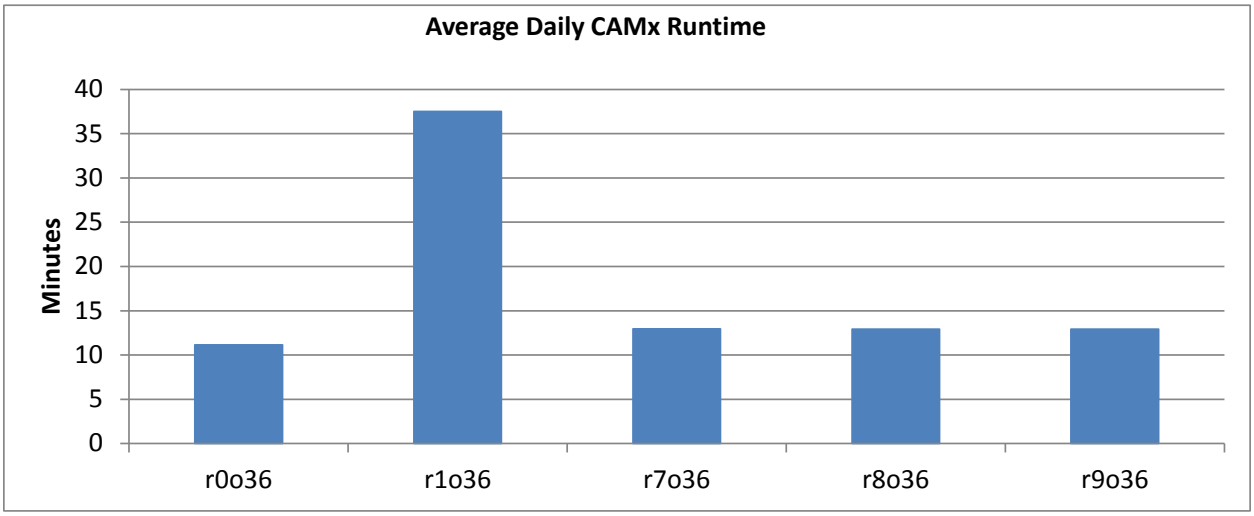

Figure 3-3. Average daily CAMx runtimes (minutes) for the TCEQ Rider 8 database using OMP over 8 CPUs to run the 36 km only grid over May 31 – June 15.

18% for the new PiG chemistry cases (r7o and r9o), indicating more efficiency gains when new PiG chemistry is used with OMP parallelization.

When running the 36 km grid alone with OMP, runtime speeds are very fast yet introduction of the original PiG leads to the largest relative increase in runtime by more than a factor of 3 (Figure 3-3). Introducing the new chemistry returns runtimes to nearly the no-PiG speed.

The much longer runtimes in the MPI tests illustrate the sensitivity of model speed to the amount of puff memory to be passed by MPI and to puff load imbalances node-to-node. The

MPI parallelization technique divides the grid into sub-domains and distributes each to a different processor that independently marches the model forward in time. The entirety of all puff memory is distributed to each sub-domain but each sub-domain processes only those puffs they possess. Those domains with large puff populations require longer runtimes and become the time-limiting processes. This results in latency as other processes must wait at the end of each time step to allow the system to synchronize before starting the next step. OMP does not suffer from such latency as all CPUs are continually tasked with puff chemistry as they become available, and OMP does not require the entirety of all puff memory to be passed among each processor. OMP is clearly more efficient in these simple 8-CPU tests and responds better to the specific PiG populations defined in the TCEQ Rider 8 configuration. But OMP is limited to the number of CPUs available on the chipset, and so OMP scalability is an issue for PiG. Currently, an MPI/OMP mix, configured according to application-specific testing, is the most efficient approach to run CAMx with a large number of PiG sources. In the future, improved MPI efficiency could be achieved through better management and passing of dynamic puff memory, and through load balancing of puff populations across the available processors.

3.2 Chemical Responses

A series of single-grid (36 km) CAMx runs were conducted with various PiG configurations to investigate ozone and NOy responses. These tests are listed in Table 3-1 as the "rXo36" series. While the main intent of using the 36 km grid was to maximize the number of runs that could be completed quickly, they were also the best way to identify and evaluate plume chemical responses since the PiG has the largest effect on coarse grids.

Figure 3-4 displays simulated hourly ozone in the no-PiG run (r0o36) on a high ozone day in eastern Texas (4 PM on June 13, 2006). Figures 3-5 through 3-7 show the chemical impacts of PiG for ozone, NO_2, and HNO_3, respectively, relative to the no-PiG run. Results from several cases are shown:

(1) Original PiG treatment distributed with CAMx v5.41 (r1o36);

(2) New PiG chemistry, in which the background chemistry step is bypassed, no background/grid contributions other than ozone, CO, and HCHO are included in the puffs, and puff gas-phase chemistry is treated with the new condensed mechanism (r7o36);

(3) New PiG chemistry with reduced nighttime minima on growth rates (r8o36);

(4) New PiG chemistry, reduced nighttime growth, and a new option to dump puff mass to coarse grids well before the reach sizes commensurate with cell size (r9o36).

Compared to no-PiG runs, PiG has typically led to minor (<10 ppb) surface ozone differences, which are usually confined to the local area around the point sources. The upper left panel in Figure 3-5, which shows the ozone difference between original PiG and no PiG cases, conforms to the typical response. Implementation of the new PiG chemistry alone, i.e. without modifications to puff growth, does not change this behavior significantly (Figure 3-5, upper

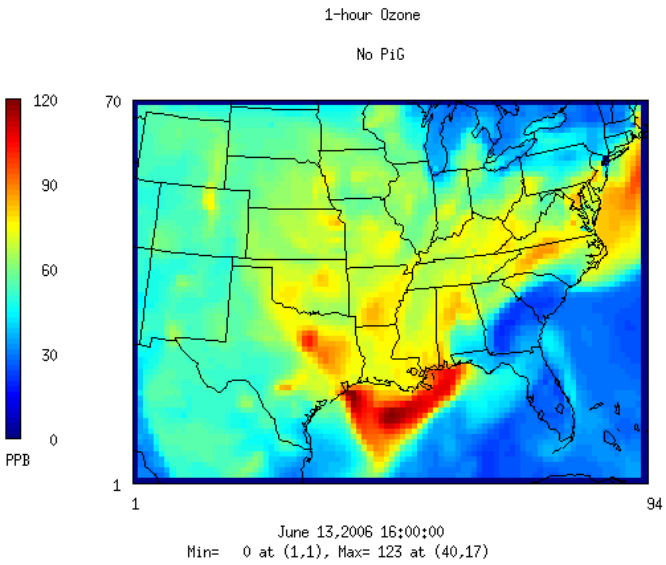

Figure 3-4. Simulated ozone in the 36 km single-grid no-PiG run at 4 PM on June 13, 2006.

right). However, there is a reduction in the number of grid cells where ozone is substantially reduced, and more areas of ozone increases. This may be related to improved nitrogen conservation, but is more likely caused by the revised chemical dumping criterion, which dramatically alters the behavior of the puff population over the day. Reducing nighttime puff growth tends to enhance the positive ozone impacts with little change to the negative ozone impacts (Figure 3-5, bottom panels). Reduced puff growth rates dramatically increase the number of puffs overnight by almost a factor of two while extending average puff ages from about 2 hours to 6 hours. Regardless, CAMx runtimes were marginally impacted by 1% or less.

While we generally believe that the new PiG chemistry results in a more proper ozone response, we remain concerned that the largest ozone impacts are associated with the lack of interaction between puff-sequestered and background NOy, especially for older, more expansive puffs that cover significant fractions of coarse grid volumes. For that reason, we introduced a new parameter to control the maximum puff size (to trigger dumping) that operates similarly to an existing parameter that controls maximum puff age. In the final run (r9o36) we set the maximum puff size limit to 10 km, meaning that any puffs reaching that size would immediately dump to the grid. We chose this as the default size limit based on the conceptual argument that the puff coherency assumption is increasingly invalid approaching and exceeding such scales. This modification led to negligible impact to the ozone results (Figure 3-5, lower right panel).

Impacts to NO_2 and HNO_3 during morning fumigation (10 AM) on June 13, 2006 are shown in Figures 3-6 and 3-7, respectively. While patterns of PiG vs. no-PiG differences are consistent between the original and new PiG treatments, in this particular test the new PiG tended toward

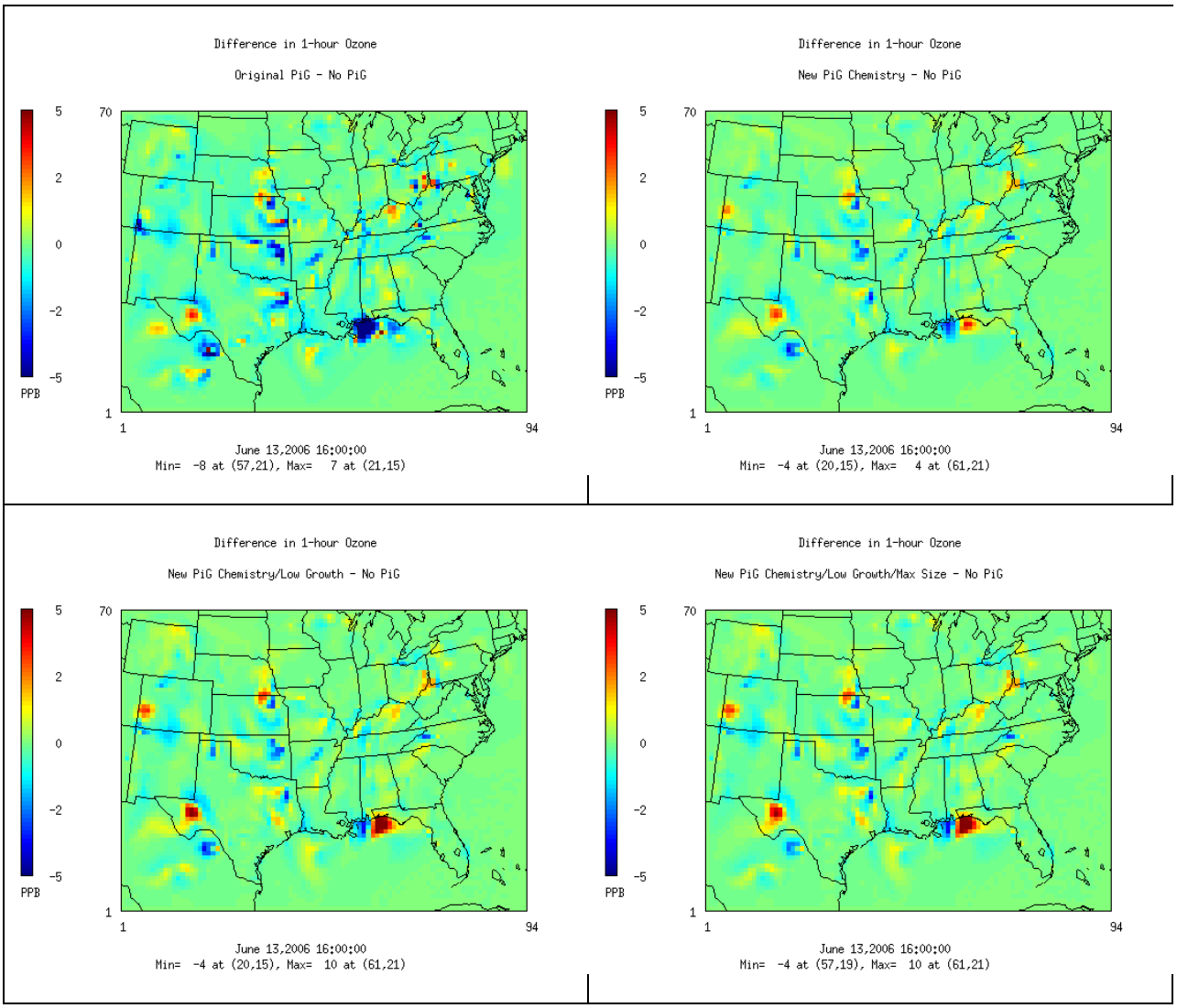

Figure 3-5. Ozone responses to different PiG configurations in 36 km single-grid test runs at 4 PM on June 13, 2006. (Top left) ozone difference resulting from original PiG; (top right) ozone difference resulting from new PiG chemistry; (bottom left) ozone difference resulting from new PiG chemistry with reduced puff growth rates; (bottom right) ozone difference resulting from new PiG chemistry, reduced puff growth rates, and maximum puff size.

less NO_2 and NOz deficits than the original PiG. This is likely a combined result of the updated chemical dumping criterion and reduced puff growth rates, which extended chemical production of NOz for several additional hours. The effect is more pronounced for longer-lasting puffs traversing coarser grids (e.g., 36 km) and minimal for finer resolutions where puffs are terminated by size constraints well before meeting chemical constraints. Again, little effect is seen from limiting puff size to 10 km.

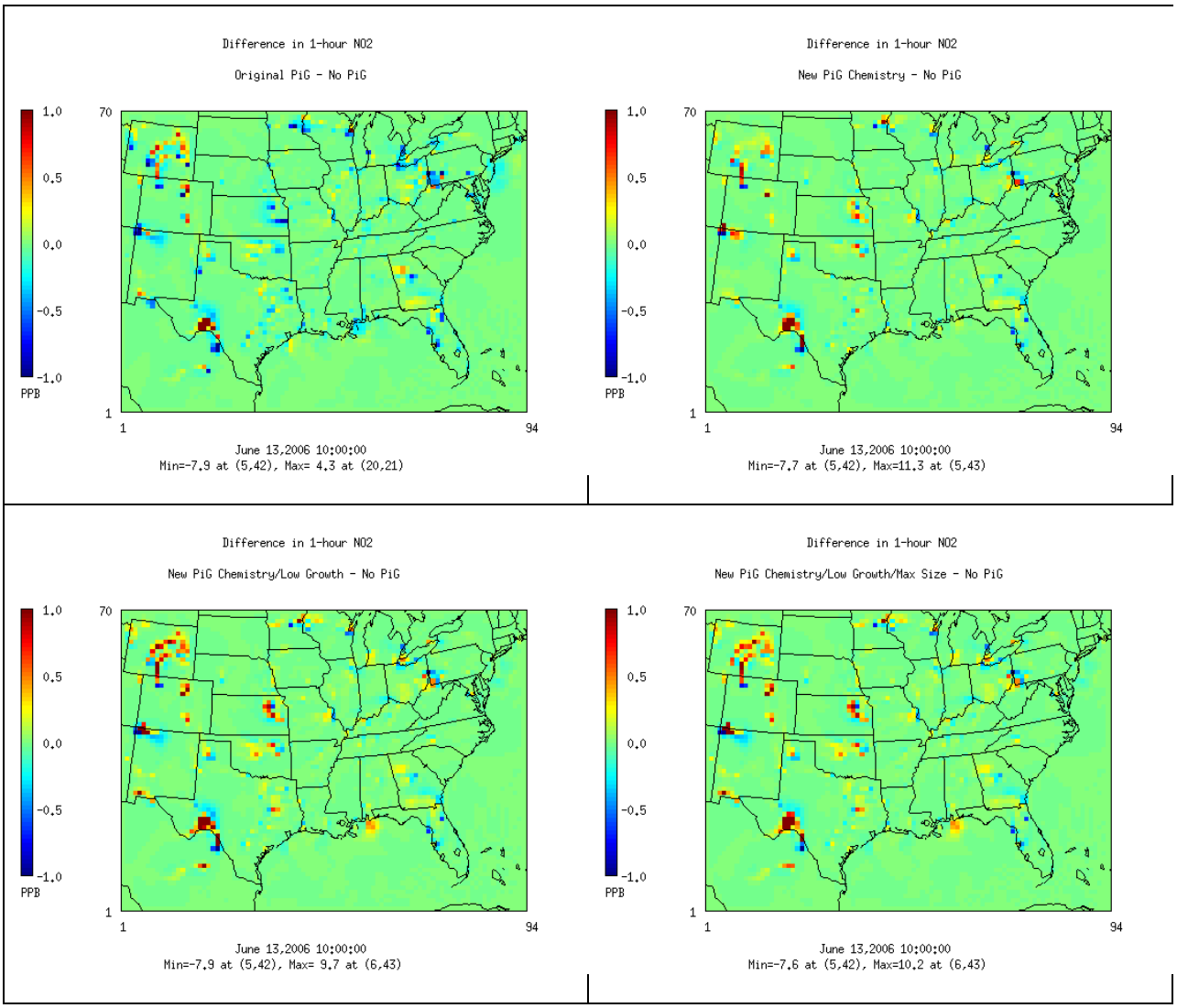

Figure 3-6. NO_2 responses to different PiG configurations in 36 km single-grid test runs at 10 AM on June 13, 2006. (Top left) NO_2 difference resulting from original PiG; (top right) NO_2 difference resulting from new PiG chemistry; (bottom left) NO_2 difference resulting from new PiG chemistry with reduced puff growth rates; (bottom right) NO_2 difference resulting from new PiG chemistry, reduced puff growth rates, and maximum puff size.

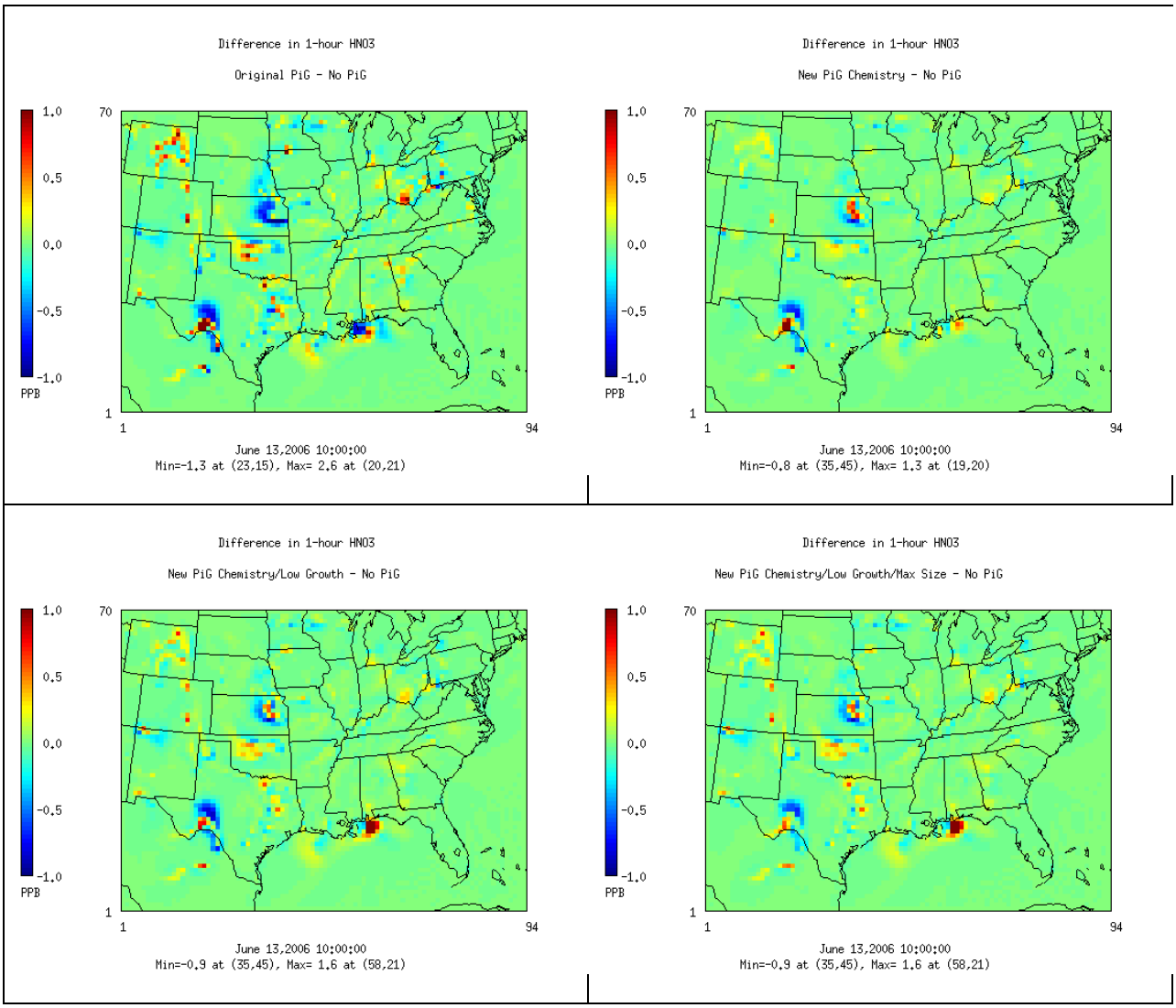

Figure 3-7. HNO_3 responses to different PiG configurations in 36 km single-grid test runs at 10 AM on June 13, 2006. (Top left) HNO_3 difference resulting from original PiG; (top right) HNO_3 difference resulting from new PiG chemistry; (bottom left) HNO_3 difference resulting from new PiG chemistry with reduced puff growth rates; (bottom right) HNO_3 difference resulting from new PiG chemistry, reduced puff growth rates, and maximum puff size.

Figures 3-8 through 3-10 show PiG vs. no-PiG impacts for ozone (at 4 PM on June 13), NO_2 and HNO_3 (at 10 AM on June 13), respectively, on the 4 km Texas grid from the nested 36/12/4 km runs. All PiG cases exhibit minor ozone impacts on the 4 km grid with slightly more ozone production from plumes with reduced nocturnal growth rates. NO_2 and HNO_3 impacts are similarly more positive in the reduced growth rate case. We also note that the new PiG chemistry with reduced growth rates eliminated the unrealistic 100+ ppb ozone spike in east Texas at 8 AM on June 13 as was reported by ENVIRON (2012).

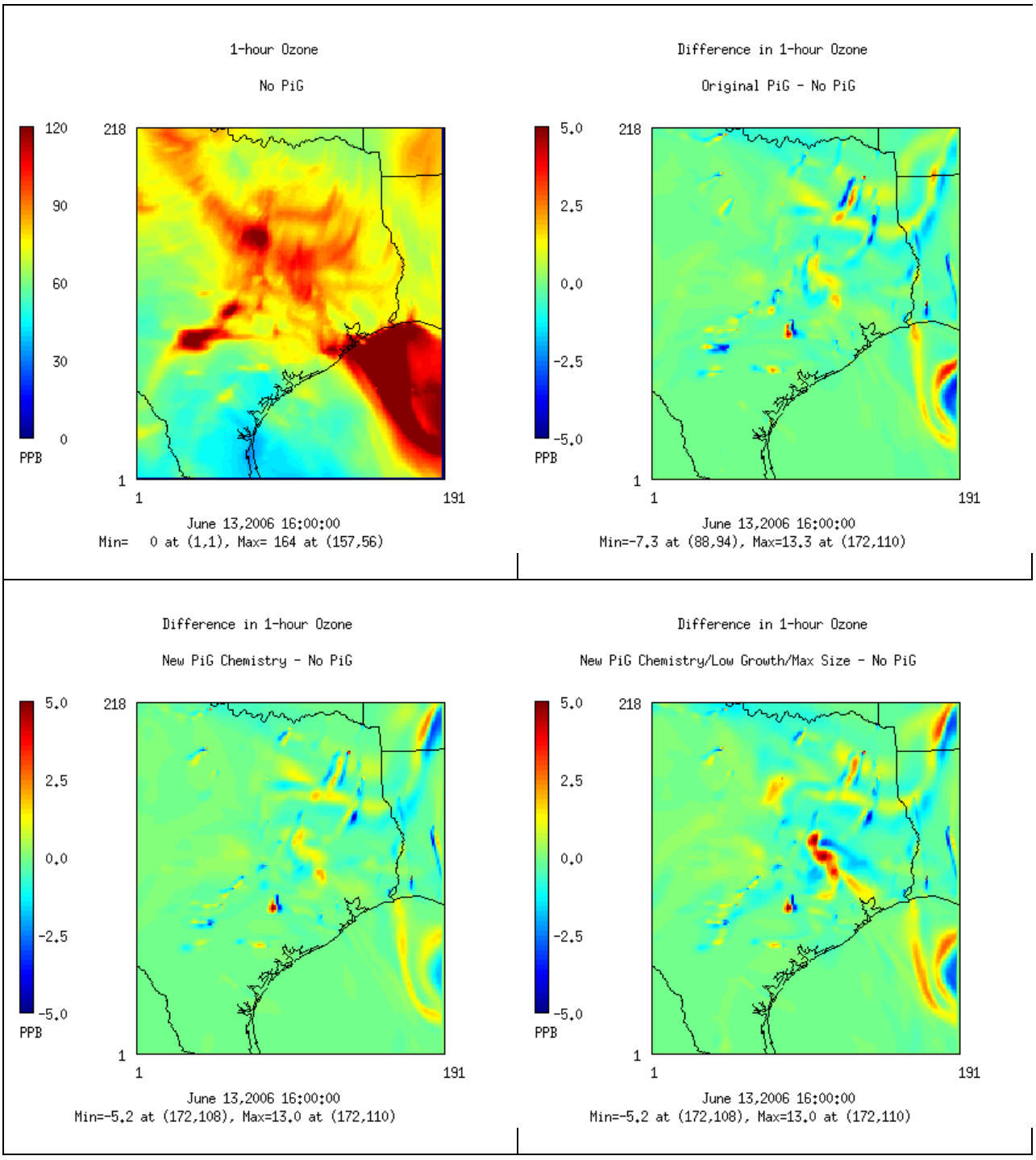

Figure 3-8. Ozone responses on the 4 km grid to different PiG configurations in 36/12/4 km test runs at 4 PM on June 13, 2006. (Top left) ozone simulated in the no-PiG case; (top right) ozone difference resulting from original PiG; (bottom left) ozone difference resulting from new PiG chemistry; (bottom right) ozone difference resulting from new PiG chemistry with reduced puff growth rates and maximum puff size.

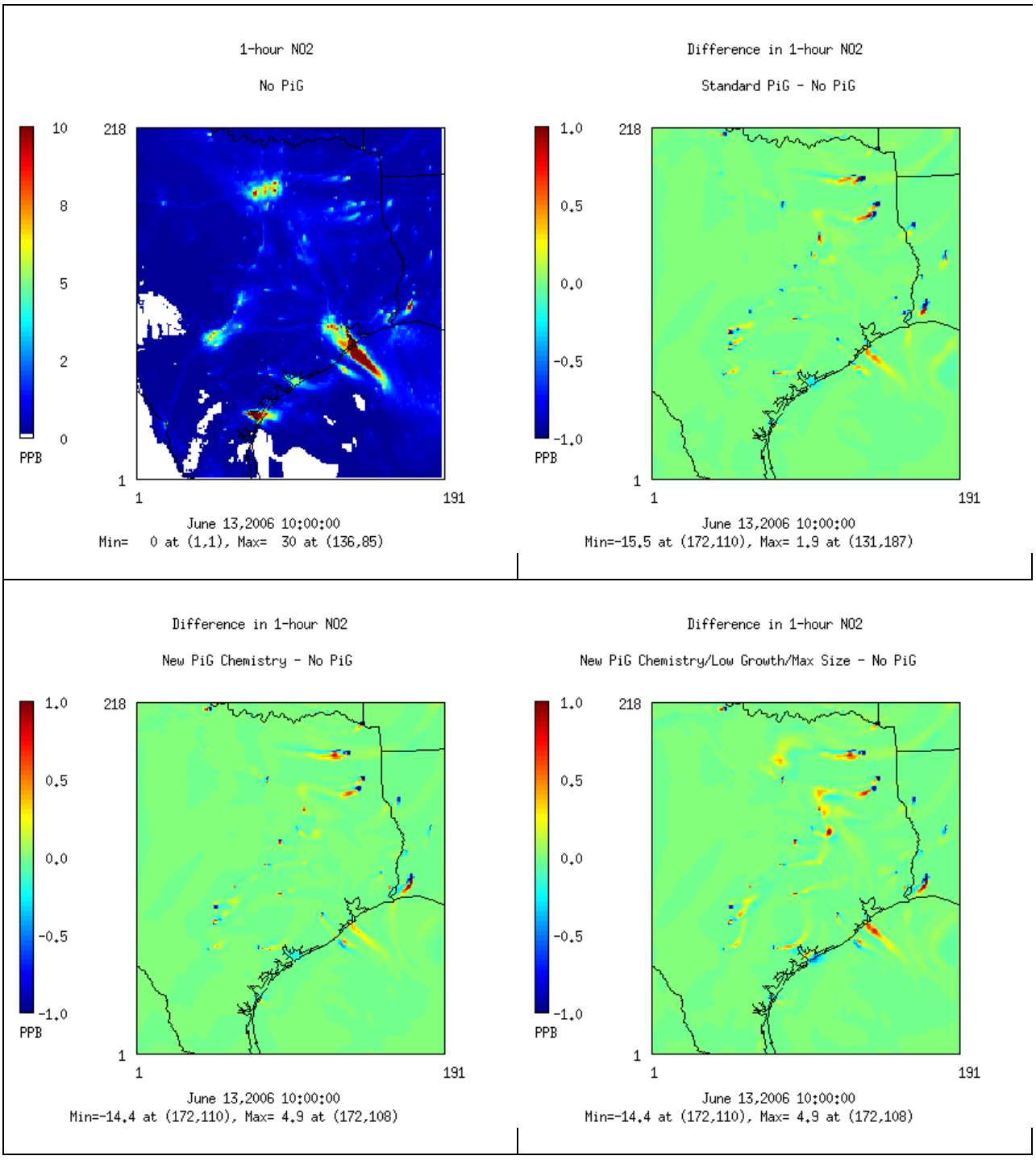

Figure 3-9. NO_2 responses on the 4 km grid to different PiG configurations in 36/12/4 km test runs at 10 AM on June 13, 2006. (Top left) NO_2 simulated in the no-PiG case; (top right) NO_2 difference resulting from original PiG; (bottom left) NO_2 difference resulting from new PiG chemistry; (bottom right) NO_2 difference resulting from new PiG chemistry with reduced puff growth rates and maximum puff size.

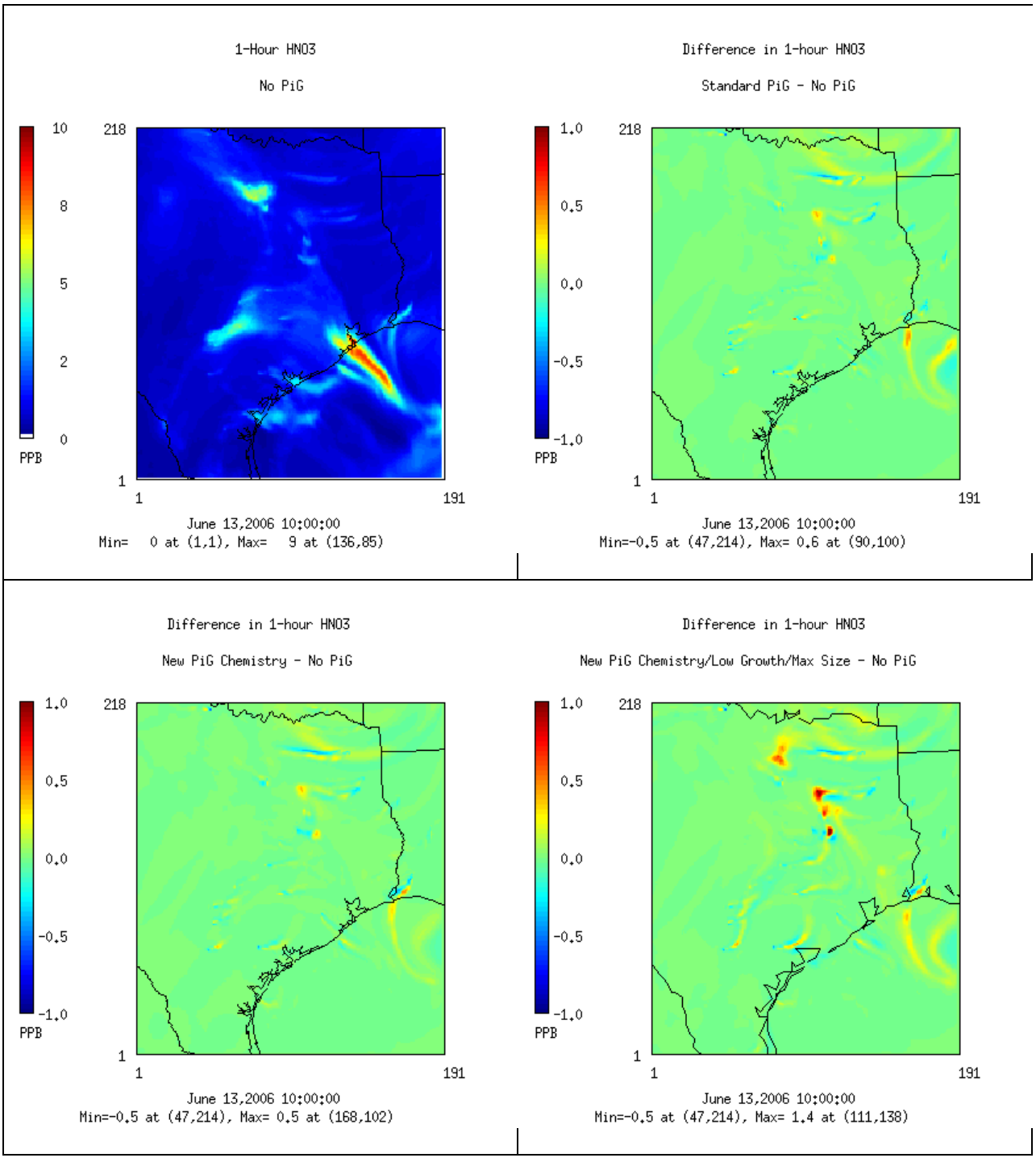

Figure 3-10. HNO_3 responses on the 4 km grid to different PiG configurations in 36/12/4 km test runs at 10 AM on June 13, 2006. (Top left) HNO_3 simulated in the no-PiG case; (top right) HNO_3 difference resulting from original PiG; (bottom left) HNO_3 difference resulting from new PiG chemistry; (bottom right) HNO_3 difference resulting from new PiG chemistry with reduced puff growth rates and maximum puff size.

Given relatively minor impacts from these PiG updates, we expected negligible impact to model performance statistics. Indeed, when we compared daily model performance for 1-hour ozone during June 1-15 over all rural east Texas monitors (not shown), bias and error statistics differed by less than 1%.

3.3 Testing the Oklaunion Plume Case

Yarwood et al. (2012) describe modeling of the Oklaunion power plant plume during the night of October 10-11, 2006. That modeling was repeated in this study to compare three cases: (1) the original CAMx v5.41 PiG; (2) new plume chemistry, including removal of the background chemistry step, no contributions from background (grid) concentrations other than ozone, CO, and HCHO, and the new condensed chemistry mechanism; and (3) new plume chemistry along with reductions in minimum nighttime growth rates.

Figure 3-11 displays a snapshot at 10 PM on October 11 of the entire train of puffs emanating from Oklaunion and heading southward for roughly 2 hours consistent with aircraft observations (this figure was replicated from Figure 4-5 from Yarwood et al. [2012]). Puff widths are symmetrically defined as $\pm 1.5\sigma$ about the puff centerline (3σ total width), where σ is one standard deviation of a Gaussian distribution. Plume growth in the original v5.41 PiG is quickest just after release, and slows dramatically after 30 minutes. The plume is consistently between 5 and 10 km wide out to 2 hours, which is wider than observed in aircraft transects at similar distances downwind that suggest plumes no wider than about 1 km according to a full width half maximum (FWHM) metric. FWHM is roughly equivalent to a 2σ ($\pm 1\sigma$) plume width, but reducing the PiG puff widths by a factor of 2/3 to account for this difference is clearly insufficient to match the measured widths.

A super high-resolution flexi-nest with 200 m grid spacing was employed by Yarwood et al. (2012) to explicitly simulate the evolution of the Oklaunion plume in lieu of the PiG model. The high resolution plume was consistently about 1 km wide within an hour of release (as defined by NOx FWHM) and slowly grew to several km wide well downstream. This was in much better agreement with the aircraft transects (see Figures 4-7 and 4-8 in Yarwood et al. [2012]).

The PiG case with reduced minimum nighttime horizontal puff growth rates shows much improvement in matching the plume width from the explicit high-resolution run. Puff sizes grow very slowly up to about 2 km after 1 hour of transport time and up to about 3 km after 2 hours. Scaling to the FWHM metric results in plume widths of 1.3 to 2 km, which is very similar to measured widths from aircraft measurements. Vertical puff spread was well replicated and so vertical puff growth rates were not modified (ENVIRON, 2012).

Figure 3-12 compares the chemical evolution of the entire ~2 hour PiG puff streams shown in Figure 3-11 (10 PM) as incremental concentrations relative to grid background. Results from all three PiG cases are shown, along with plume-averaged measurements from aircraft transects 13 and 14 at about 14 and 30 km downwind of Oklaunion (roughly 35 and 80 minutes of modeled transport time, respectively). Transect averages are also expressed as incremental

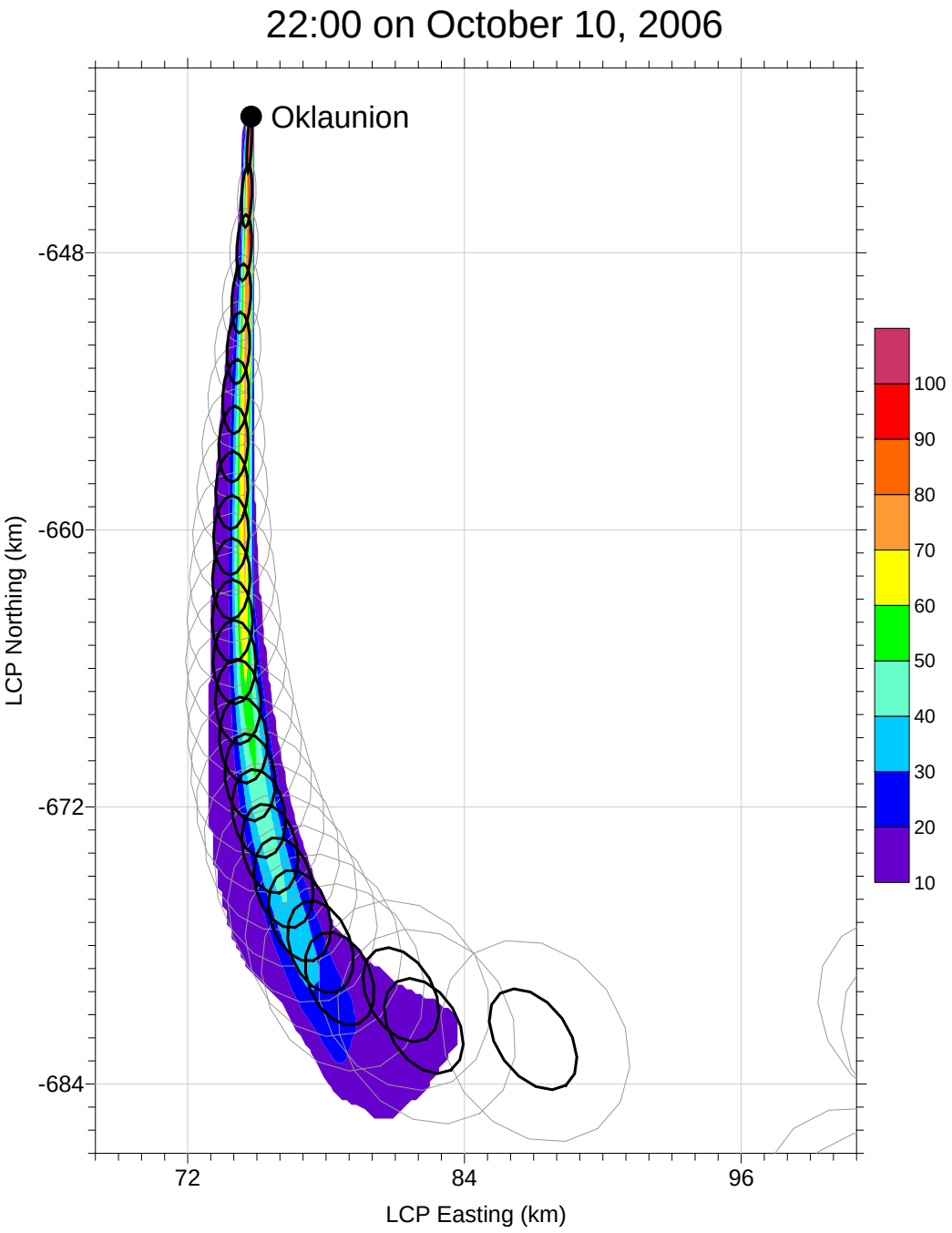

Figure 3-11. Comparison of the train of CAMx PiG puff dimensions (ellipses) against the super-high resolution NO_2 plume (colored contours in ppb) in CAMx layer 5 at 10 PM on October 10, 2006. Grey puffs are those from the original v5.41 PiG, and the smaller black puffs are the result of reducing minimum nighttime growth rates as described by ENVIRON (2012).

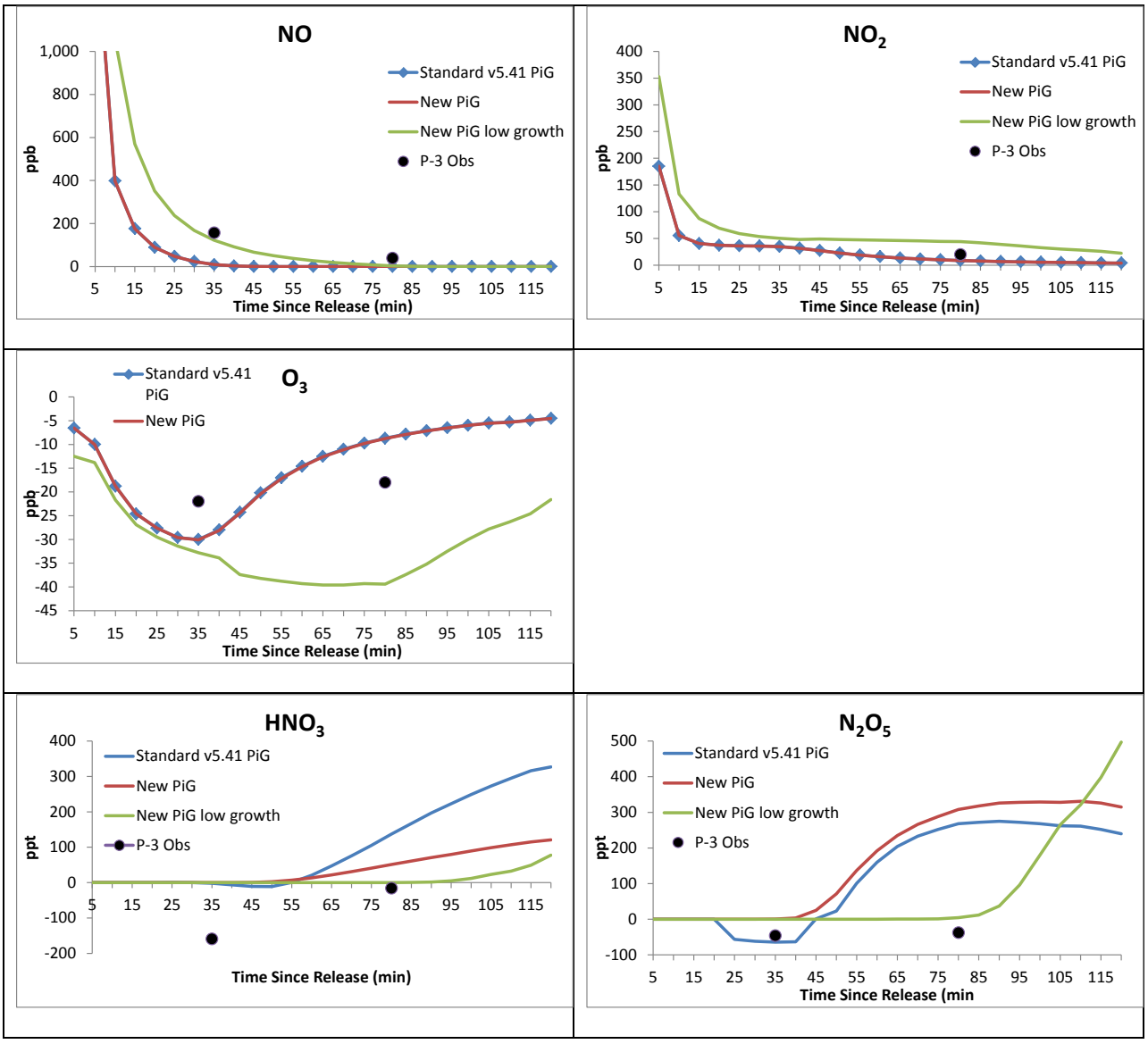

Figure 3-12. Chemical evolution in the stream of puffs from Oklaunion at 10 PM on October 10, 2006. Results from three PiG simulations (colored lines) are compared to cross-plume averaged aircraft measurements at transects 13 and 14 (black dots). All simulated and measured concentrations are shown relative to ambient background.

concentrations relative to background measurements well outside the plumes. We defined the plume widths for the calculation of transect averages according to the cross-section of measured NO concentrations clearly above background (>10 ppb). For both transects resulting plume widths were about 1 km. There is uncertainty associated with the plotted aircraft values because of our subjective definition of plume width and related sensitivity of the averages.

Modeled NOx and ozone concentrations were identical between the original PiG and new chemistry cases, which indicates that the primary conversion of NOx along the plume is correctly modeled with the condensed mechanism. NOx in the reduced growth case remained more concentrated in the smaller puff volumes. Aircraft NO measurements indicate better agreement with the reduced growth case but this is not so clear for NO_2. Ozone may be the likely cause of the discrepancy between observed and modeled NO_2. Plume ozone deficits of 30 to 40 ppb are simulated in the various PiG cases, but only 20 ppb deficits were measured. Simulated background ozone was about 40 ppb while measured background was about 25 ppb, so in reality nearly half the ozone was available to convert NO directly to NO_2. This explains the higher measured NO and lower NO_2 than simulated in the PiG even with reduced growth rates. Nevertheless, the reduced growth case extends higher NOx and negative ozone increments farther downwind in better agreement with measurements.

Turning to plume production of NOz (HNO_3 and N_2O_5), all three PiG cases vary. The original PiG allows for negative NOz increments as background contributions are involved in PiG chemistry. Both NOz components go negative in the original PiG case during the latter half of the first hour, but they remain at zero in the new chemistry case as designed. Aircraft measurements also show negative plume increments, especially for HNO_3, but this is more likely related to conversion to aerosol nitrate which is not treated by PIG. The production of NOz increases in both the original PiG and new chemistry cases at about 1 hour downwind. The new chemistry case squelches HNO_3 production but slightly increases N_2O_5 production relative to the original PiG. The reduced growth case suspends NOz production until late in the second hour. Aircraft measurements suggest no generation of plume NOz at the two transects shown, which further supports reducing plume growth rates in these tests.

Figures 3-13 and 3-14 show the evolution of total NOx and total NOz increments, respectively, along with the relative contributions from their component species. Again the evolution of NOx is identical between the original PiG and new chemistry cases, whereas the reduced growth case extends higher NO concentrations farther downwind and squelches conversion to NO_2. The NOz plots show that the new chemistry case reduces the production of total NOz somewhat, but generates a larger proportion of N_2O_5 and much less HNO_3. The onset of NOz production in the reduced growth case is much later but the N_2O_5 production rate is larger than any other PiG test.

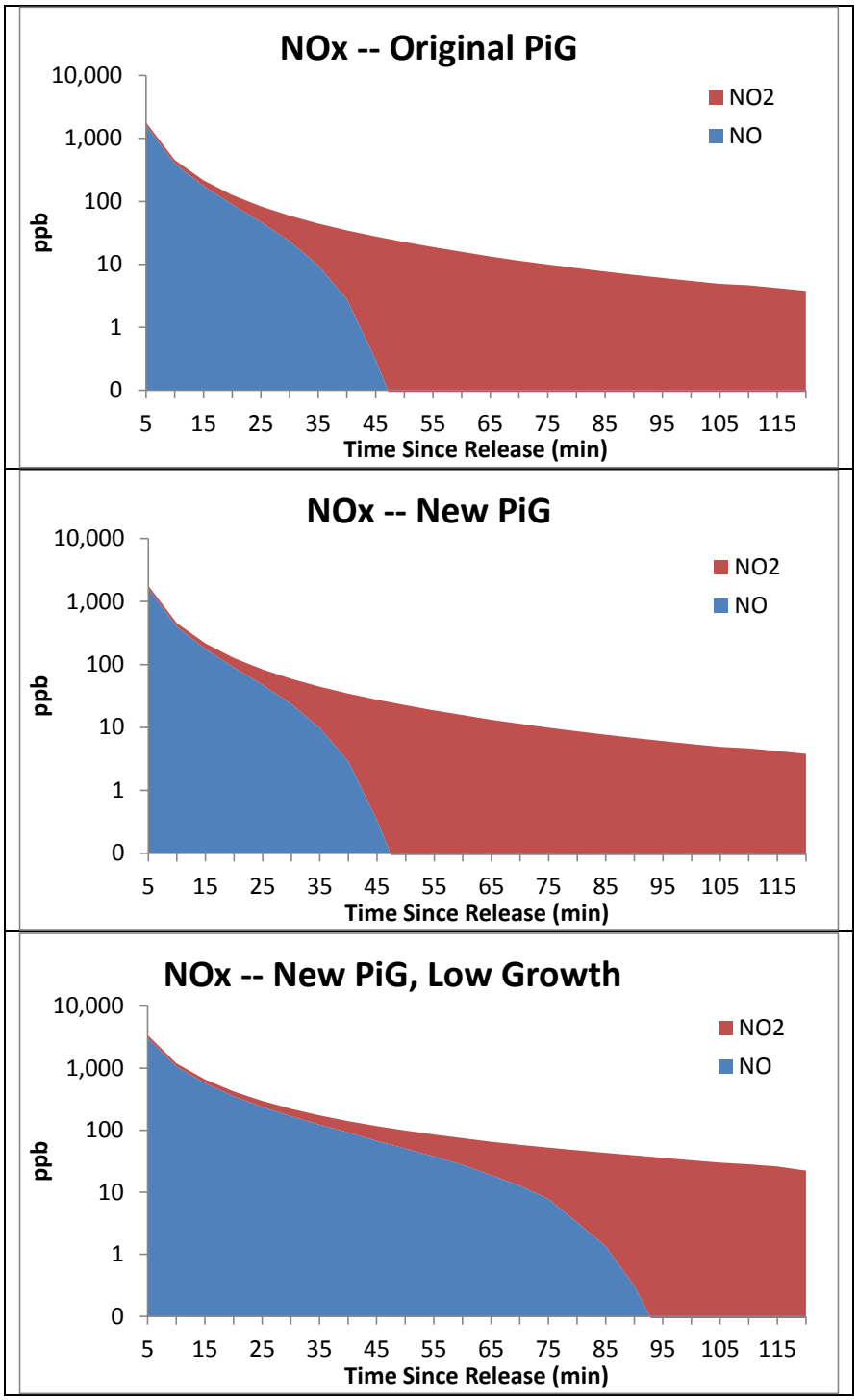

Figure 3-13. Evolution of NOx in the stream of puffs from Oklaunion at 10 PM on October 10, 2006.

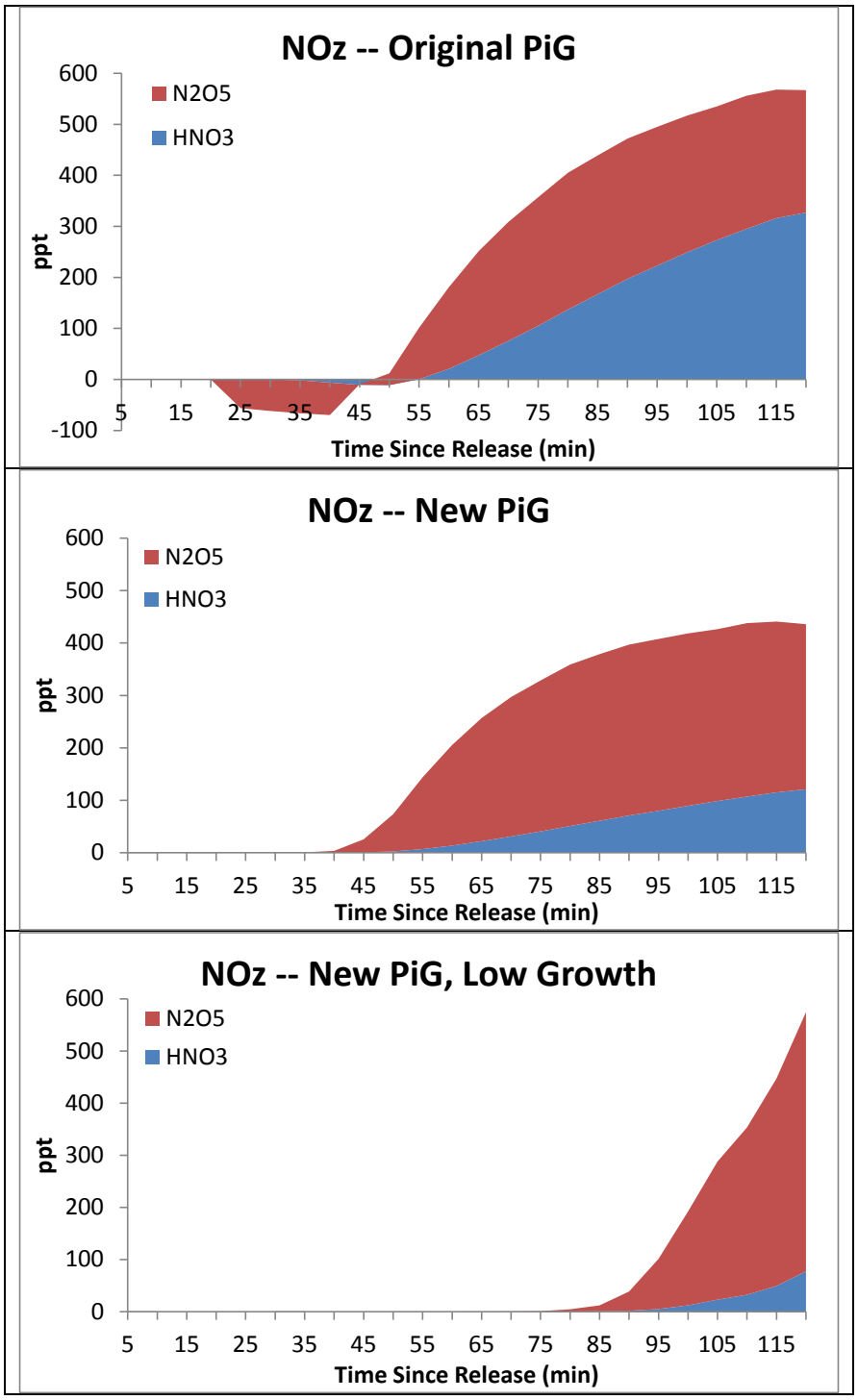

Figure 3-14. Evolution of NOz in the stream of puffs from Oklaunion at 10 PM on October 10, 2006.

4.0 CONCLUSION AND RECOMMENDATIONS

We improved the computational efficiency of GREASD PiG by developing a condensed chemical mechanism that is applicable to conditions when high NOx concentrations suppress oxidant production. With improved PiG stability, we were further able to incorporate reductions on puff growth rates that we had developed in a prior TCEQ project in 2012. CAMx sensitivity tests were conducted to analyze the effects of the modifications relative to the unmodified version of CAMx.

Box-model tests with full CB05 gas-phase chemistry revealed a gain in total oxidized nitrogen (NOy) by as much as 30% after 4 simulation hours in nighttime tests. Some of the excess nitrogen was NO_2, which could form O_3 the following day. We attributed the nitrogen non-conservation to the approach of solving puff chemistry as an increment on top of the ambient background. Sensitivity tests with the ambient background NOy set to zero demonstrated nearly perfect nitrogen conservation.

A condensed mechanism for GREASD PiG was developed that includes 23 reactions, which can be run in tandem with any of the full photochemical mechanisms available in CAMx (CB05, CB6 variants, or SAPRC99). Rate constants and photolysis rates for GREASD PiG reactions are taken directly from corresponding reactions in the grid chemical mechanism, which ensures consistency. Box model tests showed good agreement for NO, NO_2 and O_3 concentrations between the condensed mechanism and CB05. The condensed mechanism continues to be solved using LSODE. Additional modifications included: (1) skipping the "background" chemistry step, and (2) excluding all background contributions except for ozone, CO, and HCHO.

CAMx testing was conducting using pre-existing CB05 modeling datasets. Initial CAMx PiG testing using MPI and OMP parallelization was conducted using the TCEQ Rider 8 database. In both cases, the new PiG chemistry mechanism reduced total CAMx runtimes by 10-20% for the 36/12/4 km nested configuration, and by nearly 70% for a single 36 km grid configuration. The tests with MPI took much longer than OMP with the same number of processors because of differences in the parallelization approaches. An MPI/OMP mix, configured according to application-specific testing, is currently the most efficient approach to run CAMx with a large number of PiG sources.

Compared to no-PiG runs, PiG has historically led to minor (<10 ppb) surface ozone differences, usually constrained to the local area around the point sources. Implementation of the new PiG chemistry did not change this behavior significantly. Reducing nighttime puff growth tended to enhance the positive ozone concentration impacts with little change to the negative ozone impacts. Reduced puff growth rates dramatically increased the number of puffs overnight by almost a factor of two while extending average puff ages from about 2 hours to 6 hours. Regardless, CAMx runtimes were marginally impacted by 1% or less. While patterns of PiG vs. no-PiG differences in NO_2 and HNO_3 were also consistent between the original and new PiG treatments, the new PiG tended toward less NO_2 and NOz deficits than the original PiG. This is likely a combined result of the updated chemical dumping criterion and reduced puff growth

rates, which extended chemical production of NOz for several additional hours. The effect is more pronounced for longer-lasting puffs traversing coarser grids (e.g., 36 km) and minimal for finer resolutions where puffs are terminated by size constraints well before meeting chemical constraints.

While we believe that the new PiG chemistry results in a more proper ozone response, we remain concerned that the largest ozone impacts are associated with the lack of interaction between puff-sequestered and background NOy, especially for older, more expansive puffs that cover significant fractions of coarse grid volumes. For that reason, we introduced a new parameter to limit the maximum puff size (and trigger dumping) that operates similarly to an existing parameter that limits maximum puff age. The original puff size criterion that terminates puffs when they reach grid scales was modified to apply the new maximum size limit. We chose to set the default size limit to 10 km based on the conceptual argument that the puff coherency assumption is increasingly invalid approaching and exceeding such scales. This modification led to negligible impact to the ozone results.

Given relatively minor ozone impacts from these PiG updates, we verified negligible impact to daily model performance statistics for rural sites throughout east Texas. The new PiG chemistry with reduced growth rates eradicated the unrealistic 100+ ppb ozone spike in east Texas at 8 AM on June 13 as was reported by ENVIRON (2012), indicating that the approach is more computationally stable.

The new GREASD PiG was compared to data collected by aircraft in nighttime flights over Texas downwind of Oklaunion power plant. The condensed PiG chemical mechanism performed similarly to CB05. Reducing the minimum nighttime horizontal puff growth rates for PiG better matched the aircraft-observed plume width and the chemical conversion of NOx to NOz. Vertical puff spread was well replicated and so vertical puff growth rates were not modified (ENVIRON, 2012). The revised nighttime puff growth rates are implemented in the new GREASD PiG.

ENVIRON is providing the updated CAMx v5.41 code to the TCEQ for additional testing. The final GREASD PiG configuration includes the following modifications as standard features:

- The 23-reaction condensed chemistry mechanism , with rates tied to the chosen grid chemistry (CB05, CB6 variants, or SAPRC99);
- No background chemistry step;
- No inclusion of background NOy in puffs, but ozone, CO, and HCHO remain as “incremental” species;
- Reduced minimum nighttime/stable horizontal growth rates (from work performed in 2012 – also applies to IRON PiG);
- Maximum puff size constraint (10 km) for use on coarse grids (also applies to IRON PiG);

Appendix A provides an updated CAMx User's Guide section on the PiG submodel that describes the theory and rationale for PiG, physical and chemical treatments, and configuration options.

On the basis of the testing described above, we recommend future work to improve the PiG's MPI dynamic memory management, message passing efficiency, and puff load-balancing among the processors.

5.0 REFERENCES

ENVIRON, 2012. "Dallas-Fort Worth modeling support: Improving vertical mixing, Plume-in-Grid, and photolysis rates in CAMx." Final report to the TCEQ, Work Order 582-11-10365-FY12-06 (August 2012).

EPRI, 2000. SCICHEM Version 1.2: Technical Documentation. Final report prepared by ARAP/Titan Corporation, Princeton, NJ, for EPRI, Palo Alto, CA. December 2000 (1000713).

Gillani, N.V. and J.E. Pleim. 1996. "Sub-grid-scale features of anthropogenic emissions of NOx and VOC in the context of regional Eulerian models." *Atmos. Environ.*, **30**, 2043-2059.

Karamchandani, P., A. Koo, C. Seigneur, 1998. "Reduced gas-phase kinetic mechanism for atmospheric plume chemistry." *Environ. Sci. Technol.*, **32**, 1709-1720.

Kumar, N. and A.G. Russell. 1996. "Development of a computationally efficient, reactive sub-grid-scale plume model and the impact in the northeastern United States using increasing levels of chemical detail." *J. Geophys. Res.*, **101**, 16737-16744.

Yarwood et al., 2012. "NOx reactions and transport in nighttime plumes and impacts on next-day ozone." Final report for the Texas Air Quality Research Program, Project 10-020 (January 31, 2012), http://aqrp.ceer.utexas.edu/viewprojects.cfm?Prop_Num=10-020.

ENVIRON

APPENDIX A
Revised CAMx User's Guide Section
Plume-in-Grid Submodel

6. PLUME-IN-GRID SUBMODEL

Photochemistry is a highly non-linear problem because chemical reaction rates among most compounds depend upon their ambient concentrations. In Eulerian air quality models, ambient concentrations depend on how well the modeling grid resolves emissions, transport, and chemical history. Thus, grid resolution plays a vital role in the ability of the model to properly characterize photochemical conditions. Increasing resolution should in theory lead to a better model as the time/space discretization tends toward a continuum. However, practical and theoretical considerations suggest that the lower limit on horizontal grid spacing is about 1000 meters for Eulerian air quality models such as CAMx. Nevertheless, even higher resolution is often necessary to adequately simulate chemistry within concentrated point source plumes.

Some current photochemical models contain plume-in-grid treatments that track individual plume segments (or puffs) in a Lagrangian sense, accounting for plume-scale dispersion and chemical evolution until such time as puff mass can be adequately represented within the larger grid model framework. Then the puff mass is added to the grid system as a virtual source, and that mass is subsequently carried by the grid model processes. It is important to understand that the inclusion of a Lagrangian puff model within an Eulerian grid model is a forced construct. The formulations of the two modeling approaches are fundamentally different and there is no theoretically "correct" methodology.

Historically there have been two schools of thought regarding the appropriate times at which to transfer puff mass into the host model grid system. The first primarily considers the physical size of puffs relative to grid cells; once puff mass is dispersed to scales that are adequately resolved by a grid, that mass should be transferred. The two principle problems associated with this approach are deciding what the appropriate size criteria are to be, and how to distribute puff mass into the grid system. The second considers chemical evolution of the puffs (e.g., Gillani and Pleim, 1996) to find a balance between aging plume constituents adequately and sequestering plume mass from grid processes for too long. The main problem with this approach is identifying chemically mature plume mixtures within ever-evolving puffs relative to ever-evolving grid chemistry. Puffs may reach a stage of chemical maturity after very long simulation periods (say 24 hours), however it is unrealistic to assume that puffs should maintain physical coherence with no influence on grid chemistry over such time scales.

The CAMx Plume-in-Grid (PiG) sub-model addresses both chemical and size considerations. Two PiG options are available that vary in their chemical complexity. Both approaches share common design features for puff initialization, puff structure, transport, and growth. They deviate in how they treat chemistry and when they transfer mass from puffs to grid cells. This section details the structure and functionality of both options.

The first PiG approach is aimed at treating the early chemical evolution of large NO_x plumes when mostly inorganic gas-phase reactions are operative. The method is called the Greatly Reduced Execution and Simplified Dynamics (GREASD) PiG. The streamlining employed in this version was based upon our experiences in developing, utilizing, and studying the responses of

more detailed PiG algorithms for large NOx plumes. The GREASD PiG model works with the Ozone and Particulate Source Apportionment Technology (OSAT/PSAT). This is possible because of the simplified approach used in GREASD PiG and because compatibility with the source apportionment Probing Tools was an explicit design objective.

The second approach treats the full suite of gas-phase photochemistry for all types of point sources and so by necessity incorporates much more chemical complexity than the first. This CAMx plume treatment is called the Incremental Reactions for Organics and NOx (IRON) PiG. Gas-phase chemistry is simulated within each plume segment using an "incremental chemistry" approach, whereby puffs carry the incremental contributions of the puff relative to the grid concentrations. Incremental puff concentrations can be positive or negative, depending upon the species and stage of plume evolution. A similar chemistry approach is used in the SCICHEM Lagrangian model (EPRI, 2000). IRON PiG supports the Reactive Tracer (RTRAC) Probing Tool, but it does not work with the source apportionment Probing Tools and it does not treat PM.

6.1 CAMx PiG Formulation

6.1.1 Basic Puff Structure and Diffusive Growth

Both GREASD and IRON PiG sub-models share a common physical structure and growth algorithm. A stream of plume segments (puffs) is released from a designated point source. Each puff possesses a longitudinal length and directional orientation defined by the separation of a leading and a trailing point. Initial separation of these points is determined by the wind vector at final plume rise. Each point is then subsequently and independently transported through the gridded wind fields, which directly accounts for puff stretching and changes to centerline orientation due to deforming shears. The "position" of each puff is defined at the center point of each puff between the endpoints, and is used to identify the grid cell in which the puff resides for the calculation of diffusive growth and chemistry.

Like other puff models, the shape of each puff is characterized by a spread tensor, which is defined from a set of Gaussian standard deviations (σ) along the three spatial axes (σ_x, σ_y, σ_z). Diffusive growth is described by the evolution of these values. The total cross-sectional width extends $\pm 1.5\sigma_y$ from puff centerline. Similarly, the total cross-sectional depth extends $\pm 1.5\sigma_z$ from puff centerline (with limits placed on depth by the ground and by capping stable layers aloft). The total longitudinal length is the distance between the puff endpoints with an additional $\pm 1.5\sigma_x$ added in each direction. Horizontal area and total volume are calculated using the formulae for an ellipse. Figure 6-1 presents a schematic representation of each puff in horizontal cross-section.

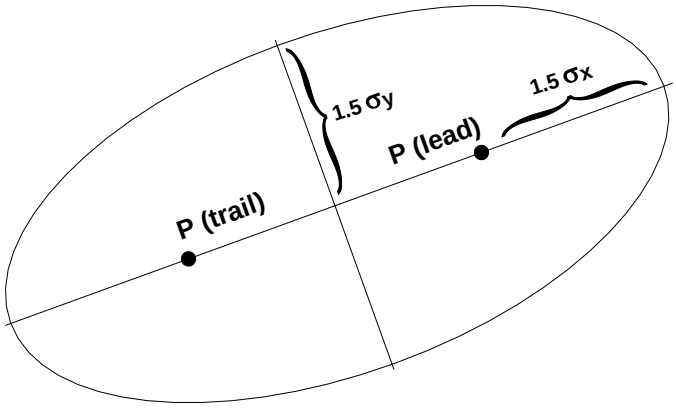

Figure 6-1. Schematic representation of CAMx PiG puff shape in the horizontal plane. Directional orientation of the puff is arbitrary, and evolves according to wind direction, shears and diffusive growth along its trajectory.

We have developed an explicit solution approach for puff growth that shares SCICHEM theory and concepts (EPRI, 2000), but includes some simplifications. SCICHEM solves predictive spatial moment equations with second-order closure that relate the evolution of the puff spread tensor ($\sigma_{ij}=\sigma_i \times \sigma_j$) to resolved mean shears and turbulent velocity statistics. The Reynolds-averaged second-moment transport equation is given as

$$\frac{d\sigma_{ij}}{dt} = \sigma_{ik}\frac{\partial \overline{u}_j}{\partial x_k} + \sigma_{jk}\frac{\partial \overline{u}_i}{\partial x_k} + \frac{\left\langle x_i' \overline{u_j' c'} \right\rangle}{Q} + \frac{\left\langle x_j' \overline{u_i' c'} \right\rangle}{Q}$$

where $\overline{u}$ is the mean wind vector component, the primed values represent turbulent fluctuations from the mean, and the angle brackets denote integrals over space. The Reynolds averaging process always introduces higher-order fluctuation correlations, and this is given by the turbulent flux moments $\left\langle x' \overline{u'c'} \right\rangle$, where $\overline{u'c'}$ represents the turbulent flux of concentration. It is these last two diffusion terms that SCICHEM solves in its second-order closure scheme.

For sub-puff scale turbulence, SCICHEM employs the restriction that the only active off-diagonal component of $\left\langle x' \overline{u'c'} \right\rangle$ is the symmetric horizontal term (i=x, j=y), but it is applied only for the large-scale (meso to synoptic) contribution to puff deformation when puff scales reach such dimensions. In CAMx, we ignore this off-diagonal flux moment term altogether since puffs are ultimately terminated when puff scales approach much smaller grid scales (typically <50 km).

SCICHEM also makes the assumption that the horizontal turbulence is isotropic, $\left\langle x'\overline{u'c'}\right\rangle = \left\langle y'\overline{v'c'}\right\rangle$.

This results in a single diffusivity equation for both *x* and *y* directions, and a single diffusivity for the *z* direction:

$$K_x = K_y = \frac{\left\langle y'\overline{v'c'}\right\rangle}{Q}$$

$$K_z = \frac{\left\langle z'\overline{w'c'}\right\rangle}{Q}$$

In our approach for CAMx, we have adopted the SCICHEM second-order tendency equations to model the time-evolution of puff turbulent flux moments (represented by diffusivities K_x=K_y and K_z) and their contribution to the evolution of puff spread (represented by the diagonal components of the puff spread tensor, σ_x^2, σ_y^2 and σ_z^2). Puff spread is defined for puff depth (σ_z), puff width (σ_y), and puff length (σ_x). We account for the effects of grid-resolved shears of horizontal wind in the evolution of lateral and longitudinal spread. But we assume that the evolution of vertical spread is solely the result of turbulent fluxes, which are orders of magnitude larger than grid-resolved shears of vertical wind.

The resulting two Reynolds-averaged second-moment transport equations for CAMx PiG are:

$$\frac{d\sigma_z^2}{dt} = 2K_z$$

$$\frac{d\sigma_y^2}{dt} = 2\sigma_y^2 D + 2\sigma_y\sigma_z S_y + 2K_x$$

$$\frac{d\sigma_x^2}{dt} = 2\sigma_x^2 D + 2\sigma_x\sigma_z S_x + 2K_x$$

where *D* is total explicit (grid-resolved) horizontal shear of horizontal wind (i.e., “deformation”, see Section 4.5). *S* is the explicit vertical shear of horizontal wind, which is broken down into puff-relative lateral and longitudinal components:

$$S_y = \left|\cos(\theta-\phi)\right|\left(\frac{du}{dz}^2 + \frac{dv}{dz}^2\right)^{1/2}$$

$$S_y = \left|\sin(\theta-\phi)\right|\left(\frac{du}{dz}^2 + \frac{dv}{dz}^2\right)^{1/2}$$

The difference between θ and ϕ represents the relative angle between the puff's longitudinal orientation and the direction of vertical shear; a cross-puff shear results in more lateral spread while along-puff shear results in more longitudinal spread. The explicit shear terms containing *D* and *S* may be toggled by the user: (1) shear effects may be applied to puff growth rates at all times; (2) shear effects may be applied only during neutral/unstable conditions; or (3) shear effects are never applied.

The SCICHEM tendency equation for the horizontal turbulent flux moment is

$$\frac{d}{dt}\left\langle y'\overline{v'c'}\right\rangle = Qq^2 - A\frac{q}{\Lambda}\left\langle y'\overline{v'c'}\right\rangle$$

where $A = 0.75$, $q^2 = \overline{v'v'}$, and Λ is the horizontal turbulent length scale. Separate equations are given for two different boundary layer turbulence scales (shear- and buoyancy-produced), such that

$$\left\langle y'\overline{v'c'}\right\rangle = \left\langle y'\overline{v'c'}\right\rangle_{shear} + \left\langle y'\overline{v'c'}\right\rangle_{buoyancy}$$

Within the surface-based boundary layer, the horizontal velocity variance is given by

$$q^2_{buoyancy} = 0.13\, w_*^2\left[1+1.5\exp\left(z/z_i\right)\right]$$

$$q^2_{shear} = 2.5u_*^2\left(1-z/z_i\right)$$

where u_* is the friction velocity, w_* is the convective velocity scale, z is height above the surface, and z_i is the height of the surface-based boundary layer. The horizontal turbulent length scale is given by

$$\frac{1}{\Lambda^2_{shear}} = \frac{1}{\left(0.3\, z_i\right)^2} + \frac{1}{\left(0.65\, z\right)^2}$$

$$\Lambda_{buoyancy} = 0.3\, z_i$$

In the stable boundary layer, only the shear components of q^2 and Λ are applied. Above the boundary layer, SCICHEM applies rough approximations for the velocity variance and turbulent length scale. In CAMx we have set these values to $q^2 = 0.1$ m^2/s^2, and $\Lambda = 300$ m.

The SCICHEM tendency equation for the vertical turbulent flux moment is

$$\frac{d}{dt}\left\langle z'\overline{w'c'}\right\rangle = A\frac{q_v}{\Lambda_v}\left(QK_z^{eq} - \left\langle z'\overline{w'c'}\right\rangle\right)$$

where $q_v^2 = \overline{w'w'}$, Λ_v is the vertical turbulent length scale, and K_z^{eq} is the equilibrium diffusivity. Whereas a specific equation for K_z^{eq} is formulated for SCICHEM, we have chosen to

specify the value of this parameter from the gridded fields of vertical diffusivity in CAMx. Again SCICHEM gives separate equations for shear- and buoyancy-produced turbulence scales.

Within the surface-based boundary layer, the vertical velocity variance is given by

$$q_v^2\Big|_{shear} = 1.5u_*^2\left(1 - z/z_i\right)$$

$$q_v^2\Big|_{buoyancy} = 1.1w_*^2\left(z/z_i\right)^{2/3}\left(1.05 - z/z_i\right)$$

The vertical turbulent length scale for both shear and buoyancy is equal to Λ_{shear} given above for horizontal length scale. Above the boundary layer, SCICHEM applies rough approximations for the velocity variance and turbulent length scale and we have adopted these for CAMx: q_v^2 = 0.01 m^2/s^2, and Λ_v = 10 m.

The external variables needed by PiG to complete the dispersion calculations include z_i, u_* and w_*. All of these are available from an internal module in CAMx that calculates these boundary layer similarity theory parameters. Thus, no additional parameters are needed to be input to the model.

6.1.2 Puff Transport

A fresh set of new puffs are released from all PiG point sources within the modeling domain for the duration of the smallest time step among the master and all nested grids. The length of each puff is determined by the combination of the mean total wind speed at the height of final plume rise and time step. Limits are placed on maximum extruded length based on half the finest resolution in the given simulation. If winds and time-steps are such that the maximum allowed length is violated, then several puffs are automatically emitted from a given stack per time step. The user can also set a maximum time interval of release if more puffs (better plume resolution) are desired over the default automated release interval. The orientation of the puff length is along the total wind vector. Total puff volume is determined by stack volumetric flow rate in conjunction with growth due to turbulent entrainment following the SCICHEM approach. Initially, $\sigma_x = \sigma_y$ and σ_z values are explicitly calculated from this entrainment calculation.

The effects of resolved wind shear on plume deformation (i.e., at plume scales larger than individual puff scales) are treated using a "chained puff" approach (Figure 6-2). Points at the leading and trailing edges of the puff centerline are individually transported through the gridded wind fields, which directly accounts for puff stretching and changes to centerline orientation due to deforming shears. Since puffs can extend over multiple layers, layer density-weighted average wind components are determined for each endpoint based on the vertical coverage of the puff.

The "chain" aspect means that at least initially (as puffs are emitted from the stack) the trailing point of a puff emitted at time *t* will be the leading point of a puff emitted at time *t+dt*. However, as the puffs are advected downstream, the leading point of one puff will deviate from

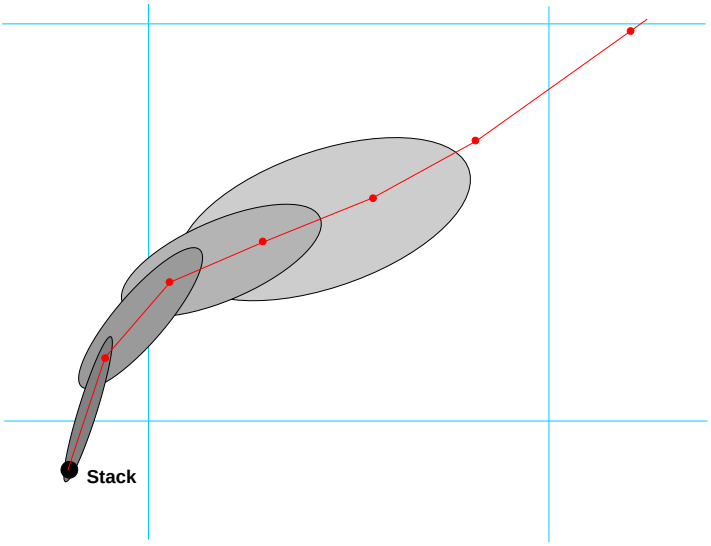

Figure 6-2. Plan-view schematic representation of a chain of PiG puffs emitted from a point source into an evolving gridded wind field. The red line connected by dots represents puff centerlines, with dots representing leading and trailing points of each puff. The CAMx computational grid is denoted by the blue lines.

the trailing point the puff behind it due to evolving puff depth and wind fields. Puff volume is conserved in convergent/divergent wind fields. Puff endpoints may move closer together or further apart, in wind fields that are slowing or accelerating downstream. We compute puff end-point separation changes and then adjust puff widths and depths to maintain constant puff volume. The change in computed puff endpoint spacing defines puff length tendencies, then puff depth tendencies are computed from grid-resolved vertical wind shear ($\partial w/\partial z$), and finally we determine the puff width tendencies required to conserve puff volume.

The "position" of each puff is defined by its center point between the endpoints. This position defines the grid domain and grid cell in which the puff resides for the calculation of diffusive growth and chemistry. This definition holds even if the puff is sufficiently long that the endpoints are in different grid cells (or even different nested grids if near a nest boundary). With our definition for termination when horizontal area approaches grid cell area, the puff length should not extend across more than two grid cells.

6.2 GREASD PiG

The GREASD PiG is designed for large NOx point sources, where only inorganic chemistry is operative during early plume evolution. The intention of GREASD PiG is to more properly age emitted NOx within the confined plume volume to mitigate the artificially rapid chemical processing of fresh NO to NO_2 to ozone that would otherwise occur if immediately released into a large grid volume. A condensed inorganic chemical mechanism is employed in GREASD PiG that includes 23 reactions involving oxidation of NOx and SOx. Therefore, GREASD PiG should not be used for VOC sources. Chemical limitations applied within GREASD PiG cause

puffs to transfer their mass to the grid before oxidant production from VOCs is no longer suppressed; this can occur before puffs reach a size threshold determined by the grid spacing.

The chemical evolution of large NOx point source plumes can be characterized in three stages (EPRI, 2000), as described below:

- Stage 1: Early plume conditions where NOx concentrations are very high and radical concentrations are negligible – simple $NO/NO_2/O_3$ photostationary state applies along with the NO-NO self reaction;
- Stage 2: Mid-range plume conditions where radical concentrations are sufficiently large to generate secondary inorganic acids like nitrate and sulfate;
- Stage 3: Long-range plume conditions where sufficient mixing with the ambient air leads to the full range of gas-phase reactions involving VOC oxidation and ozone formation.

The objective for GREASD PiG is to transfer mass to the grid at about the time when radical production via organic chemistry starts to become important, so GREASD PiG treats plume chemistry during Stages 1 and 2. We define the onset of Stage 3 chemistry when the following criterion is met:

$$\frac{k_{OH}[CO] + k_{OH}[SO_2]}{k_{OH}[NO_2]} > 1$$

At this point GREASD puffs transfer all of their mass to the grid before the onset of Stage 3. This specific design constraint is also compatible with the requirements of the source apportionment Probing Tools.

Kumar and Russell (1996) and Karamchandani et al. (1998) found that PiG models with simplified inorganic chemistry produced results that were very similar to full chemistry. The chemical mechanism for GREASD PiG includes 23 reactions listed in Table 6-1 that were selected as follows:

- Reactions for the NO-NO2-O3 photo-stationary state established in sunlight (1-3)
- Self-reaction of NO important only at very high NO concentrations (4)
- Production of OH by photolysis of O3 and HONO in sunlight (5-9)
- Production of nitric acid in sunlight (10)
- Formation of NO3 and N2O5 at night (11-17)
- Production of nitric acid at night (18)
- Production of sulfuric acid in sunlight (19)
- Removal of OH by CO (20)
- Production of OH by photolysis of formaldehyde (21-22)
- Conversion to OH of any HO2 formed in 20-22 (23)

Table 6-1. List of 23 reactions for GREASD PiG including correspondence to CAMx reaction numbers in the CB05, CB6 and SAPRC99 mechanisms.

Chemical Mechanism for GREASD PIG		Corresponding Reaction Number for Grid Chemistry		
Number	Reaction	CB05	CB6	S99
1	NO2 = NO + O	1	1	1
2	O + O2 + M = O3 + M	2	2	2
3	O3 + NO = NO2	3	3	7
4	NO + NO + O2 = 2 NO2	22	24	10
5 [1]	NO + NO2 + H2O = 2 HONO	23	41	N/A
6	O3 = O1D	9	9	18
7	O1D + M = O + M	10	10	20
8	O1D + H2O = 2 OH	11	11	19
9	HONO = NO + OH	25	43	22
10	NO2 + OH = HNO3	28	45	25
11	NO2 + O3 = NO3	7	26	8
12	NO3 = NO2 + O	14	27	16
13	NO3 = NO	15	28	15
14	NO3 + NO = 2 NO2	16	29	9
15	NO3 + NO2 = NO + NO2	17	30	14
16	NO3 + NO2 = N2O5	18	36	11
17	N2O5 = NO3 + NO2	21	37	12
18 [2]	N2O5 + H2O = 2 HNO3	19	39	13
19	SO2 + OH = SULF + HO2	63	52	44
20	OH + CO = HO2	66	123	29
21	FORM = 2 HO2 + CO	75	97	123
22	FORM = CO	76	98	124
23	HO2 + NO = OH + NO2	30	25	31

1. Rate for GREASD PiG reaction 5 set to zero when used with SAPRC99.
2. Rate for GREASD PiG reaction 18 may be enhanced by reaction on aerosol.

These reactions dominate gas-phase chemistry in plumes from major NOx emitters during stages 1 and 2. Table 6-1 also shows the correspondence between GREASD PiG reactions and the complete gas-phase chemical mechanisms implemented in CAMx, namely CB05, CB6 and SAPRC99. This mapping is used in CAMx to set the rate constants and photolysis rates for GREASD PiG reactions from corresponding reactions in the grid chemical mechanisms. This implementation ensures consistency with these chemical mechanisms.

The GREASD PiG performs gas-phase chemistry for only those chemical species emitted directly into the plume, and does not include the influence from any background compounds on the grid except for ozone, carbon monoxide, and formaldehyde. Assuming zero background for gas

species is reasonable for the early stages of NOx plumes because puff concentrations are orders of magnitude larger than ambient concentrations. On the other hand, background ozone, carbon monoxide, and formaldehyde are the primary sources of oxidants in the condensed mechanism that drive inorganic processing of plume NOx to other forms of oxidized nitrogen (NOz), so these are handled as "incremental" species as described below for IRON PiG. The Livermore Solver for Ordinary Differential Equations (LSODE) is used to solve the condensed mechanism in double-precision, regardless of the user-chosen solver employed for the grid chemistry.

6.3 Particulate Matter In PiG

Non-linear effects and errors in gas-phase chemistry are transmitted to (and potentially amplified by) the PM aqueous chemistry and partitioning algorithms. The implementation of PM and PSAT in PiG prompted the need to limit the impact of such issues similarly to the constraints imposed by OSAT for gas-phase chemistry. Therefore, PM and PSAT can only be run using the GREASD PiG option. As for gas-phase chemistry, only inorganic PM chemistry is treated by GREASD PiG.

The GREASD PiG gas-phase chemistry oxidizes NOx and SOx emissions to nitric and sulfuric acids, which are PM precursors. To maintain consistency with the grid chemistry, aqueous PM chemistry (RADM-AQ) is then performed at every time step if the puff resides in a cloudy grid cell. However, inorganic gas/PM partitioning (performed by ISORROPIA) among sulfate, nitrate and ammonia is not performed by GREASD PiG, but is delayed until the masses of these compounds are dumped to the grid. Additionally, chemistry and partitioning for secondary organic aerosols is not performed.

Note that the PiG PM treatment was designed specifically for the static 2-mode PM chemistry only (CF), and will not operate for the multi-section PM chemistry (CMU).

6.4 IRON PiG

The IRON PiG model incorporates a complete treatment of gas-phase chemistry in point source pollutant plumes, while secondarily adding additional features central for treating toxic pollutants not normally carried by the standard CAMx chemical mechanisms. Therefore the IRON PiG can treat a wide variety of point source emissions, including VOC sources.

Several approaches have been developed to treat photochemistry within point source plume models. One of the more elegant methodologies is the incremental chemistry idea embodied in the SCICHEM model (EPRI, 2000). However, we found that the implementation of incremental chemistry in SCICHEM is very complex, especially in its handling of the chemistry of overlapping puffs, and is not sufficiently flexible to allow for the adaptation of numerous chemistry mechanisms and solvers.

We adopted the incremental idea for IRON PiG whereby each puff carries concentrations relative to ambient background. This results in the possibility of both positive and negative puff concentrations depending on how the chemistry evolves. The full gas-phase chemistry mechanism chosen for a given run (CB05, CB6 or SAPRC99) is solved twice for each puff at each time step: first for the vertically-averaged background concentrations from the grid cells vertically spanned by the puff; and second for the sum of puff and background concentrations. The LSODE solver is used to solve both chemistry steps, regardless of the user-chosen solver employed for the grid chemistry. After both steps are completed, the updated background concentrations are subtracted from the updated puff+background concentrations, yielding the new puff incremental concentrations. These new puff increments are subsequently advected and dispersed by the transport portions of the PiG code.

Note that the updated background concentrations, which may include "virtual dumps" of mass from large overlapping puffs (described below), are used for reference only in the puff incremental chemistry algorithm; the actual grid concentrations are not affected and are separately solved by the grid chemistry routine.

6.5 PiG Features

This section describes specific features of the PiG submodel; certain features are always active while others can be optionally invoked for a particular CAMx run. The IRON PiG sub-model includes two constructs designed specifically to facilitate the incremental chemistry approach:

- The concept of "virtual dumping" to handle the chemical impacts of large puffs that can overlap other puffs within a given grid column;
- The concept of multiple puff "reactor" cells to account for the chemical effects of concentration distributions within each puff.

Each of these is described below.

6.5.1 Puff Layer Spanning (IRON and GREASD)

The PiG is designed to chemically process point source plume mass within streams of puffs until such time that each puff can be adequately resolved on the horizontal grid. Puffs are allowed to vertically span multiple grid model layers before they reach horizontal grid scales. This introduces technical implications for defining "background" concentrations and ambient conditions for puff chemistry, as well as for transferring plume incremental mass to the grid. The solution employed is to:

1) Assume that the vertical distribution of puff concentration is always uniform;
2) Distribute puff mass transfer (via "leaking" and "dumping") to the grid according to the puff fractional coverage across each model layer and by density-weighting; and
3) Determine mean background concentrations and other ambient conditions (e.g., temperature, humidity, etc.) over the puff vertical span via similar fractional layer-density weighting.

Horizontally, the mean background concentration and ambient conditions are taken from the single host grid column containing each puff center point, even if the puff is large and/or spans a horizontal cell interface. As described earlier, puffs are considered to be elliptical in the horizontal, with the minor axis spanning the cross-wind puff width (defined as $\pm 1.5\sigma_y$), and the major axis spanning the along-wind puff length (defined as length $\pm 1.5\sigma_y$ on each end). However, given the complications associated with multiple layers spanning and mass-weighting of ambient inputs and dumped mass, puffs are rectangular and uniform in the vertical, with total puff depth defined as $\pm 1.5\sigma_z$.

6.5.2 Puff Overlap and the Idea of Virtual Dumping (IRON only)

The chemical effects of puff overlap were considered to be an important attribute of IRON PiG. However, we wished to maintain a relatively simple approach, while appropriately accounting for the largest probable effects. We assume that the largest effect is the condition in which older expansive puffs span significant fractions of their host grid cell, thereby potentially overlapping all other puffs contained within the same cell. Instead of geometrically determining fractional overlap puff-by-puff, we instead introduce a process that we refer to as "virtual dumping."

For a given grid column, the mass from all puffs determined to be "sufficiently" large are temporarily dumped to the column, distributed according to each puff's vertical layer span, and added together along with the pre-existing grid concentrations. This process is referred to as a "virtual dump" of puff mass to the grid column. The criteria to determine a "sufficiently" large puff is the same that initiates puff mass leaking to the grid (as described below). In this approach, all large puffs contribute to the background chemistry step for other puffs occupying the same grid column. Double-counting is avoided by not including a puff's contribution to the background while its specific background and incremental chemical calculations are performed.

6.5.3 Multiple Puff Reactors (IRON only)

Accounting for full chemistry potentially introduces significant non-linear effects that are highly dependent upon the distribution of pollutant mass within each puff. Especially for ozone, aircraft flights through power plant plumes have often recorded wide concentration variations relative to ambient conditions: within the plume core where NOx remains concentrated, ozone is often depressed and follows NO-NO_2-ozone equilibrium, whereas on plume fringes where NOx is dilute and mixes with ambient VOC, ozone concentrations can exhibit concentration maxima. Past models have accounted for cross-plume chemistry variations through the use of reactors, with approaches ranging from multiple rectangular slabs to concentric shells.

The user may select multiple reactors as well to sub-divide the puff. Any number of reactors may be chosen (the default is 1). Multiple reactors simply divide the total puff volume evenly, and the initial mass assignments for newly emitted puffs are made using the standard error function that results in an initial Gaussian-like mass/concentration distribution among the reactors. This provides a mechanism for simulating the differing chemical processing that takes place in various concentration regimes. As the purpose of the reactors is merely to represent

the range of photochemical conditions that are likely to occur at various locations within the puff as it undergoes differential shearing and mixing, there is no particular physical orientation assigned to these reactors with respect to each other or to the puff as a whole. Thus, there is no communication (i.e., diffusional mass exchange) between the reactors. The same background concentration chemistry applies to all reactors of a given puff. When puff mass is leaked or dumped, all reactors shed the same relative fraction of mass.

In summary, chemistry is solved for each puff "reactor" in three steps:

1) The layer-mean background (grid + overlapping puff) concentrations and environmental conditions over the volume occupied by the puff are stored and then chemically updated via the LSODE gas-phase chemistry mechanism;
2) The pre-updated mean background concentrations are added to the puff increments and the total concentrations are chemically updated; and
3) The updated results from step 1 are subtracted from the updated results of step 2 to provide the updated incremental concentrations.

6.5.4 Puff Dumping (IRON and GREASD)

Mass transfer from puff to grid can happen in two ways: slowly, termed "leaking", or suddenly, termed "dumping." As described earlier, all mass is transferred to the vertical grid structure in a density-weighted fashion according to each puff's fractional layer coverage. The process of leaking ensures that puff mass is transferred to the grid continuously, rather than in discrete lumps of pollutants with very different concentrations than those in the grid. Sudden dumping can cause unphysical numerical shocks in the grid and can lead to unrealistic gridded concentration patterns that appear as "bulls eyes". The idea behind puff leakage is to account for turbulent shearing of mass from the main plume and its subsequent dispersion to the grid scale. This rate of transfer should be directly proportional to the puff size relative to the grid scale.

Puff leakage is controlled by comparing the horizontal area of a puff to a specified leakage parameter, defined as a fraction of horizontal grid cell area. When a puff is first emitted there is no leakage. As the puff grows in volume the concentrations within the reactors are reduced accordingly by dilution. When the puff area exceeds the leakage onset parameter, a fraction of the mass in each puff reactor is transferred to the grid. This fraction is determined by the relative exceedance of the leakage parameter; initial leakage is slow as the exceedance is relatively small, but leakage rates grow as the puff continues to grow beyond the leakage parameter.

The reduced mass from leakage is compensated by a reduced effective volume, so that concentrations are not artificially diluted by leakage (an essential chemical imperative). Thus, two distinct volumes are tracked: the actual volume (defined by the puff spread σ) and the effective volume. While these are identical before leakage, they deviate after leakage is

initiated, and thereafter the relative deformation of the actual puff volume (via diffusion, shearing, etc.) is used to scale the deformation of effective puff volume.

Eventually the horizontal span of the puff will exceed the grid cell area, and the remaining mass is then dumped all at once to the grid. However, because of the combination of photochemical processing and leakage, by the time a puff dumps the potential for producing numerical shocks is much reduced. Furthermore, if the puff exceeds a user-defined maximum age, puff mass is transferred to the grid at the rate of 10% per timestep.

6.5.5 PiG Rendering (IRON and GREASD)

While the mass confined to the puffs at any given time has not yet affected the grid concentrations, it will eventually, so it can be somewhat misleading to sequester this mass from visualizations of a model simulation. The puff mass can be optionally incorporated into the model average output files for visualization purposes (referred to as "PiG rendering"). Rendering employs a "virtual dump" of the puff masses into the average output concentration array each time step. As described for chemistry, virtual puff mass is added as an increment over the entire grid column according to fractional layer-density weighting over puff depth, thus diluting it's concentrations relative to that within the puff. The actual puff mass remains within each puff over the course of its lifetime, and the actual grid mass in unaffected until puffs are killed and their masses truly dumped into the grid. This visualization is available for either 2-D surface or 3-D average output files, and can produce some rather startling effects in output displays, including very narrow virtual plumes, or streaks, representing mass moving through the grid in sub-grid puffs, but not subject to grid-scale eddy diffusion.

6.5.6 High Resolution Puff Sampling (IRON and GREASD)

PiG optionally employs surface-layer puff sampling of CB05, CB6, or SAPRC99 species on a user-defined grid of arbitrary horizontal resolution, similarly to the way nested grids are defined. Sampling grids are entirely passive, and intended to provide a display of the plume concentrations at scales much smaller than typically used for the finest computational grids (i.e., <1 km), primarily around and downwind of a source complex. Sampled PiG concentrations are time-averaged like the output concentrations provided on the computational grids, and are written to files with similar format so that they may be readily viewed and manipulated with CAMx post-processing software. Additional information on configuring and using PiG sampling grids is provided in Sections 2 and 4.

Given that the puffs constantly evolve via diffusive growth and reshaping due to deforming shears, the sampling procedure includes trigonometric calculations to define which sampling points are influenced by each puff. This influence is determined according to the puffs' two-dimensional horizontal Gaussian shape shown in Figure 6-1. To include a sufficiently large percentage of mass across each puff for sampling, limits of $\pm 3\sigma_{x/y}$ in both horizontal dimensions are used to define the puffs' total elliptical area coverage. Puffs are only sampled if they extend vertically into the model's surface layer.

Sampling grids are defined in the CAMx control file (see Section 2), and array dimensions must be set sufficiently large in the CAMx Fortran parameters file in `./Includes/camx.prm` (see Section 2). An example of the type of plume detail that can be visualized using a sampling grid is provided in Figure 6-3. In this case, a very fine 200 m sampling grid is set within a 4-km computational grid.

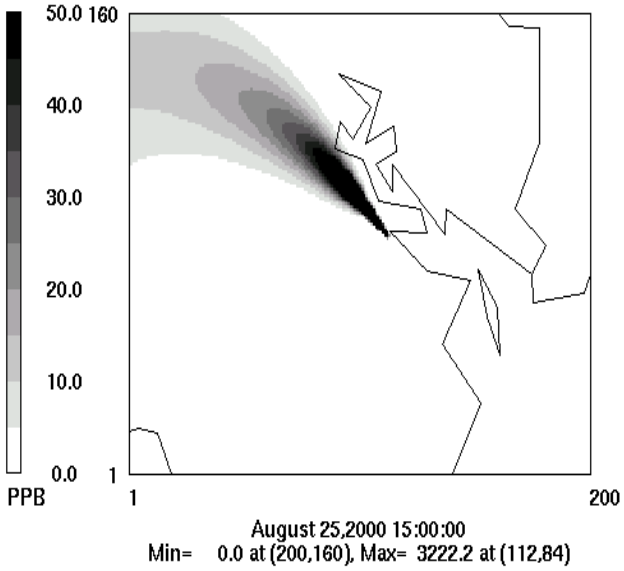

Figure 6-3. Example of a single point source PiG plume as depicted by a sampling grid with 200 m resolution (shown by the extent of the plot; 40 km by 32 km total extent). This sampling grid was set within a CAMx computational grid with 4-km resolution. The source location is arbitrary and is emitting an inert tracer.

6.6 Deposition

The CAMx PiG treats the removal of gas and PM species from each puff via deposition processes. Both dry and wet deposition calculations presented unique implementation issues for puffs. The most difficult issue for both forms of deposition was how to manage deposition exchange between puffs and the ground in the case of negative puff concentration increments.

6.6.1 Dry Deposition

Dry deposition needs to consider the following: (1) the point at which puffs begin to deposit to the surface; (2) how to handle deposition through potentially deep puffs that may straddle several layers of varying stability since the puffs do not themselves resolve these stratifications or vertical concentration distributions; (3) managing deposition fluxes of negative concentration increments. Our solution to issue (1) was to ignore dry deposition within puffs until they diffusively grow to the ground, although in reality deposition occurs on roughness elements that extend some distance above the ground (trees, buildings, etc.). We

implemented a criterion that the bottom of the puff must extend to or below the midpoint of the surface layer, or below 10 m (whichever is larger), in order for dry deposition to be active.

Issue (2) can be handled in a variety of ways and complexity. The current implementation institutes a simpler solution and we will consider more complicated improvements for future developments if evidence suggests that they would be necessary. PiG utilizes pre-computed species-dependent deposition velocities derived for the grids. Each puff in a particular grid cell is provided the host cell's deposition velocities for each species, and these are used to determine the flux of mass through the fraction of puff depth occupying the model's surface layer.

Issue (3) is unique to the incremental chemistry concept introduced with IRON PiG. The flux of material depositing to the ground is given by $F = c \cdot v_d$, where by the normal definition a positive deposition velocity v_d leads to a positive deposition flux to the ground. If the puff increment c is negative, then a negative flux is calculated (flux from ground to puff). This is appropriate if we consider the following argument. Dry deposition applied to a grid cell removes some pollutant mass from the entire volume. If there is a puff existing in that cell with a negative concentration increment, then the amount of mass removed from the cell was over estimated if we consider the puff's contribution to total cell mass. The negative deposition flux calculated for this puff leads to the addition of mass to the puff increment. Adding mass to a negative increment reduces the magnitude of the increment, as expected for a deposition process. This mass is taken from the grid cell's accumulated deposited mass to maintain accurate mass accounting within the model.

6.6.2 Wet Deposition

Wet deposition needs to consider the following: (1) how to handle scavenging of pollutants through potentially deep puffs that may straddle several layers of varying cloud and rain water contents but that do not themselves resolve vertical concentration distributions; (2) managing deposition fluxes of negative concentration increments in combination with the potential for mass to move in and out of rainwater as it falls (e.g., for slightly soluble gasses); (3) accounting for the initial pollutant concentrations in rainwater as they enter the top of each puff.

It was important to maintain consistency between the treatment of wet deposition and the approach for puff chemistry. The chemistry relies on the assumption of vertically well-mixed puff reactors that can span multiple layers, and this is why layer-density weighted average ambient conditions are passed to the chemistry routines. To maintain this assumption for wet deposition, a single scavenging rate is applied through the entire puff depth as effectively a single layer of pollutant. This was found to be the simplest implementation approach. This single scavenging rate is calculated according to layer-density weighted average ambient cloud and rainwater contents.

Wet scavenging is performed throughout the entire depth of the puff to determine the amount of flux in or out of rainwater. Total concentrations (puff + background) are used to determine

species-dependent scavenging rates using the identical algorithm as for grid removal. The rates are used to derive removal fractions, and these fractions are then applied directly to the puff incremental mass for each species. Removal fractions are considered positive for the standard case of mass moving from puff to rain. We further assume that the top boundary condition for rainwater entering the top of each puff is zero. This means that the removal fraction is always positive (from puff to rain) in the single-layer puff. In contrast, for gridded concentrations the layer-by-layer buildup of slightly soluble species can lead to a reversal of fluxes (from rain to grid) if super saturation is diagnosed in a particular layer.

Note that negative puff mass increments in combination with a positive removal fraction lead to a reversal of the flux direction (rain to puff), but that is not allowed and in such cases wet scavenging is set to zero. We account for impacts on the mass budget appropriately by adding to the wet deposition mass array according to the net fluxes into rainwater.

6.7 PiG Configuration

Selecting the individual elevated point sources to receive the PiG treatment is accomplished by setting their stack diameters negative within the header (time-invariant point list) section of the CAMx input point source file. CAMx will run correctly with these negative diameters even if the PiG algorithm is not invoked. CAMx preprocessors exist to ease the procedure of ranking elevated point sources by emission rate and flagging the sources that the user wishes to treat.

Invoking the CAMx PiG sub-model is controlled by keywords in the CAMx control file (`CAMx.in`), as described in Section 2. The choices are:

```
PiG_Submodel  = 'NONE',
PiG_Submodel  = 'GREASD',
PiG_Submodel  = 'IRON',
```

Note that the single choice between GREASD and IRON applies to all flagged point sources. It is not possible to make a single CAMx run with IRON PiG applied to a certain group of sources, and GREASD PiG applied to another group. Also note that GREASD must be selected to run PiG with OSAT, PM and PSAT; IRON must be selected to run PiG with the RTRAC Probing Tool. Several additional parameters are used to configure the PiG. It is important to note that all PiG configuration parameters exist in the CAMx Fortran parameters file (`./Includes/camx.prm`), as described in Section 2. PiG parameters are grouped together and briefly described at the end of that file. By effectively configuring the PiG submodel in the code, the default PiG configuration (as recommended by the model developers) is preset within the model distribution and alleviates the need for users to select settings on their own.

The default values are shown below:

```
parameter ( MXPIG    = 50000 )
parameter ( MXRECTR  = 1 )
parameter ( FLEAK    = .25 )
parameter ( LEAKON   = .FALSE. )
parameter ( LVISPIG  = .FALSE. )
parameter ( OVERLAP  = .FALSE. )
parameter ( DXYMAX   = -10000. )
parameter ( AGEMAX   = 18.*3600. )
parameter ( PIGMXDT  = 300. )
parameter ( SHRFLG   = 1 )
```

Users should exercise thoughtful consideration when altering these default values. A description of each of the remaining parameters is provided below, along with guidance in setting values.

6.7.1 Guidance on the Use of CAMx PiG

6.7.1.1 PiG Keyword

The PiG keyword controls whether the PiG option is to be invoked in a CAMx simulation, and whether the emissions are treated with the GREASD or IRON options. This keyword can be switched from NONE to GREASD or IRON on a model restart to invoke the PiG treatment at any point during a multi-day simulation. To allow for this, it is not mandatory to provide CAMx with a pre-existing PiG output file upon a model restart – CAMx will not stop if this file is missing. It is recommended that this file be provided on all subsequent restarts since the PiG output file is needed to reinitialize the PiG module, otherwise all mass contained in puffs at the end of the previous run will be lost. If the PiG keyword is switched to NONE on a model restart, CAMx will continue the simulation without PiG, but all mass contained in puffs at the end of the previous run will be lost.

- Guidance:
  - Invoke GREASD or IRON PiG at any point during a multi-day simulation, or none at all. Once PiG is started, provide CAMx with the PiG output file from the previous run for all subsequent model restarts so that no point source mass is lost.
  - GREASD PiG should be invoked for large NOx point sources only, since it does not provide any organic chemistry. GREASD PiG supports PM chemistry (CF, but not CMU). It can be run in conjunction with the OSAT and PSAT Probing Tools. It does not support DDM, PA, or RTRAC.
  - IRON PiG can be invoked for any point source to treat gas-phase chemical evolution using CB05, CB6 or SAPRC99 mechanisms. IRON PiG does not treat particulate chemistry. It can be run in conjunction with the RTRAC Probing Tool. It does not support OSAT, PSAT, DDM, or PA.

Both GREASD and IRON options use the LSODE chemistry solver exclusively, so users will notice a significant impact on run time, particularly if many (~thousands) puffs are to be tracked and/or IRON PiG is invoked (2 solutions of full photochemistry for each puff), and/or IRON puffs are configured with many puff reactor cells (full photochemistry solutions each). Since GREASD chemistry is simpler and the lifetime of GREASD puffs are much shorter than their IRON counterparts, GREASD PiG will run faster than IRON PiG for the same number of flagged sources. PiG chemistry is internally parallelized using OMP to maximize PiG speed performance.

6.7.1.2 Number of PiG Puffs

MXPIG sets the maximum number of PiG puffs to be expected during a simulation. It is used to statically allocate memory arrays for the PiG sub-model. A value of 10,000 is usually sufficient for most applications in which PiG is used; set this parameter to 1 if PiG is not used to conserve memory. If this parameter is exceeded during a simulation, the model will halt. If this happens, simply increase `MXPIG`, recompile the model executable, and restart the simulation.

- Guidance: Use the default value for most simulations, or set to 1 if PiG is not to be used. If the model stops because MXPIG is exceeded, increase its value, recompile, and restart the model.

6.7.1.3 Number of PiG Reactors (IRON only)

MXRECTR sets the number of puff reactors; when greater than 1, each puff is separated into that number of reactor cells and primary emissions are apportioned among them using a Gaussian distribution. Since chemistry is performed for each individual reactor cell (both background and puff+background), this parameter can affect the speed of chemical computations in the PiG. We have not seen a significant sensitivity to values greater than 1, but testing for each application is warranted.

- Guidance: Use the default of 1 for initial simulations, but test the sensitivity to this parameter for each unique application.
- Reactors greater than 1 are not allowed for GREASD PiG.

6.7.1.4 Leakage Parameters

FLEAK, LEAKON, and DXYMAX together control puff leakage to the computational grid and ultimately puff termination. When LEAKON is true, FLEAK and DXYMAX control when puffs begin to leak portions of reactor mass to the grid along their trajectory. When LEAKON is false, no leaking is performed and puffs maintain all of their mass until they reach sizes for termination, at which point all mass is directly introduced to the grid at that point. DXYMAX sets the maximum dimension that puff size will be compared to for leaking and termination: when it is zero, puff size will be compared to grid area only; when it is positive, puff size will be compared to the value of DXYMAX regardless of grid resolution; when it is negative, puff size will be compared to DXYMAX or grid resolution, whichever is smaller. FLEAK is the relative fraction of horizontal puff area to cell area (or DXYMAX) above which leaking will begin and

continue until sufficient mass is shed and the puff is terminated. In the example above, puffs will begin to leak mass when they reach 25% of the host grid cell's area.

- Guidance: If LEAKON is set to true, maintain FLEAK at the default value of 0.25. Then test model sensitivity to different values of FLEAK and/or DXYMAX.
- Guidance: We suggest leaving DXYMAX = -10000, meaning puffs will be terminated when they reach the grid scale or 10 km, whichever is smaller. Puffs exceeding this size are usually well-aged and go beyond reasonable assumptions of puff coherence (also see AGEMAX parameter below).
- Leaking is not allowed when PiG is run with PM.

6.7.1.5 Overlap Flag (IRON only)

OVERLAP controls whether puff overlap is to be treated in the background chemistry step. As stated earlier, puffs only overlap if they meet the size criteria for leaking; all puffs smaller than this size do not overlap any other puffs in the same grid cell.

- Guidance: We recommend that the OVERLAP flag remain set to the default value of "false".
- Overlap is not allowed for GREASD PiG.

6.7.1.6 Virtual Puff Rendering

LVISPIG is a flag that turns on puff "rendering" to the computational grid average concentrations. When it is false, the chemical effects of puff mass are not seen on the output average files until they either begin to leak mass to the grid and/or they are terminated and their mass is entirely introduced to the computation grid. However, when the flag is true, all puff mass that resides in each grid column is summed, apportioned vertically to each grid cell according to puff vertical extent (via density and layer-depth weighting), converted to concentrations, and added to the average gridded concentrations for output. This process is referred to as rendering since the effects of all puff mass can be readily visualized in the CAMx output.

- Guidance: This option has no impact on the actual CAMx chemical solution. However, output average concentration files will be affected by puff rendering, and therefore could impact graphics of CAMx results and model performance measures.
- Virtual dumps are not allowed when PiG is run with PM.

6.7.1.7 Maximum Puff Age

AGEMAX is the age limit for all PiG puffs (IRON and GREASD). When puffs reach this age limit, they are terminated and all of their mass is transferred to the host grid.

The assumption of a stream of coherent puffs becomes less valid with time as horizontal and vertical wind shears increase plume spread. At some point the plume mass is better resolved on the grid than within puffs. In CAMx the rate of puff expansion most often determines this

transfer of mass, and the maximum puff age provides a safety check to ensure that puffs do not persist for unrealistic times in stable environments. The maximum puff age should be set long enough to allow puffs to persist overnight, but a lifetime of longer than a day is probably not realistic.

- Guidance: limit puff age to 12-24 hours – we find that 18 hours works best since it will allow puffs emitted in the late afternoon to last through the night and into the following morning. The purpose is to restrict growth-limited puffs to terminate overnight simply as a result of age constraints. Twelve hours is seen to be too short in this regard; puffs usually do not reach 24 hours of age before being terminated by grid constraints.

6.7.1.8 Maximum Puff Release Interval

PIGMXDT sets the maximum frequency of release and by default is set to 300 seconds (5 minutes). This value should be adequate for most applications. However, if the user wishes to improve plume resolution by increasing the number of puffs, the frequency of release can be increased by reducing the value of PIGMXDT. This value supersedes the automated puff release rate that is determined by wind speed and grid size.

- Guidance: Maintain the default value of 300 s and allow PiG to use the automated PiG release frequency. Set to a lower value if better plume resolution is desired; note that more puffs will be released and this could slow the model markedly.

6.7.1.9 Effects of Wind Shear on Puff Growth Rates

SHRFLG sets the approach by which to apply the effects of explicitly resolved (grid scale) wind shear on puff growth rates. There are three options available to the user:

0 = shear is never applied;
1 = shear is applied only within the neutral/unstable boundary layer;
2 = shear is always applied.

- Guidance: The application of wind shear can lead to large growth rates, especially during stable conditions at night, and this may over-dilute puff concentrations, lead to early transfer of puff mass to the grid, and have markedly reduced impacts on next-day ozone. Shear has less relative impact on growth rates during the daytime because turbulent growth on its own leads to rapid plume dilution. For these reasons, the default is to ignore the effects of shear during the night or when puffs are above the boundary layer.